Effect of synaptic cell-to-cell transmission and recombination on the evolution of double mutants in HIV

Jesse Kreger[a], Natalia L. Komarova[a] and Dominik Wodarz[b,a]

a) Department of Mathematics, University of California Irvine, Irvine CA 92697

b) Department of Population Health and Disease Prevention Program in Public Health
Susan and Henry Samueli College of Health Sciences, University of California, Irvine CA 92697

Abstract

Recombination in HIV infection can impact virus evolution *in vivo* in complex ways, as has been shown both experimentally and mathematically. The effect of free virus versus synaptic, cell-to-cell transmission on the evolution of double mutants, however, has not been investigated. Here we do so by using a stochastic agent-based model. Consistent with data, we assume spatial constraints for synaptic but not for free-virus transmission. Two important effects of the viral spread mode are observed: (i) For disadvantageous mutants, synaptic transmission protects against detrimental effects of recombination on double mutant persistence. Under free virus transmission, recombination increases double mutant levels for negative epistasis, but reduces them for positive epistasis. This reduction for positive epistasis is much diminished under predominantly synaptic transmission, and recombination can in fact lead to increased mutant levels. (ii) The mode of virus spread also directly influences the evolutionary fate of double mutants. For disadvantageous mutants, double mutant production is the predominant driving force, and hence synaptic transmission leads to highest double mutant levels due to increased transmission efficiency. For advantageous mutants, double mutant spread is the most important force, and hence free virus transmission leads to fastest invasion due to better mixing. For neutral mutants, both production and spread of double mutants are important, and hence an optimal mixture of free virus and synaptic transmission maximizes double mutant fractions. Therefore, both free virus and synaptic transmission can enhance or delay double mutant evolution. Implications for drug resistance in HIV are discussed.

Virus evolution *in vivo* is a central characteristic of human immunodeficiency virus (HIV-1) infection [21, 15, 32]. Viral evolutionary processes have been shown to drive disease progression through a variety of mechanisms, including evolution of immune escape or evolution towards virus strains with faster replication kinetics, increased cytopathicity, and broader cell tropism [21]. A relatively high mutation rate of HIV-1 [31], together with a high turnover of the virus during the chronic phase of the infection [44, 16, 39], certainly contributes to the generation and emergence of mutants that drive this disease. These mutational processes are also implicated in the evolution of drug resistance during anti-viral therapy.

In addition to mutations, another mechanism that contributes to virus evolution is recombination [30, 20, 34]. HIV is a diploid virus containing two copies of genomic RNA. If cells are infected simultaneously by different virus strains [30], two different viral genomes can be packaged into the same virus particle. When this virus infects a new target cell, recombination between these two genomes can occur during reverse transcription, when the viral DNA is generated. Recombination has the potential to bring two separate point mutations together in a single virus genome that previously were present in different genomes. Recombination has been shown experimentally to play an important role in HIV-1 infection [34, 33] in situations where the accumulation of two or more mutations is required to achieve a given phenotypic effect. Examples are the generation of virus mutants that are simultaneously resistant against two or more drugs, or mutants that have escaped two or more immune cell clones.

The process of recombination requires the infection of cells with two or more viruses that are genetically different [30]. In HIV, the multiple infection of cells has been shown to be promoted by direct cell-to-cell transmission of the virus, through the formation of virological synapses [17, 7, 1, 42]. Many viruses are transferred simultaneously from the source cell to the target cell, several of which can successfully integrate into the new host cell, making this an efficient mode of infection. Further, experiments have shown that if cells are infected with two distinct virus strains, synaptic transmission promotes the repeated co-transmission of these different strains from one cell to the next [8, 29], which can promote the occurrence of recombination. This was demonstrated both *in vitro* [8] and *in vivo* [29] using HIV-1 infection of humanized mice. *In vivo* data also suggests that the process of synaptic transmission is spatially restricted, meaning that transmission likely occurs to neighboring target cells [29].

The effect of viral recombination on the *in vivo* evolution of HIV has been investigated with mathematical models, revealing a wealth of results, in particular in the context of drug resistant viruses. In [12], recombination was found to be detrimental to the doubly-resistant virus. In [5], the role of recombination was reported to depend on the relative fitness characteristics of single and double mutants, but for most plausible scenarios it was established that recombination slowed down the evolution of resistance. In the models of [2, 6], it was determined that recombination was beneficial for double mutants. In [28] it was clarified that the results strongly depend on the model formulation. In particular, a distinction was made between (i) population genetic (constant population) and population dynamic models, and (ii) stochastic and deterministic models. The model employed in [28] combines a population dynamic description with stochasticity, and finds that recombination decelerates the emergence of drug resistance.

In the present paper we focus on the evolutionary dynamics of double mutant evolution in HIV infection, and how this is influenced by the mode of virus spread (synaptic vs. free virus transmission) and the occurrence of recombination. Just as in [28], we use a stochastic, population dynamic model. In contrast to the above paper, however, we do not use a combined model where "pre-treatment" and "treatment" regimes are both included, but instead focus in more general terms on disadvantageous, advantageous, and neutral mutants. We consider fitness landscapes that range from maximal positive to maximal negative epistasis, expressed by a parameter that ranges from zero to one. Times to double mutant invasion and the fraction of double mutants at defined time points are recorded in the presence and absence of recombination, and for a variety of different virus transmission strategies that range from 100% synaptic to 100% free virus transmission.

1 Modeling virus evolution

1.1 Stochastic modeling of spatially restricted synaptic virus transmission

Virus dynamics can be modeled by using ordinary differential equations (ODEs) [36, 38]. Extensions of those models that include both free virus and synaptic transmission modes, as well as multiple infection have been since investigated, see [27, 24, 25, 3, 11, 10, 9].

In vivo data from humanized mice indicate that synaptic transmission results in spatial clusters of infected cells [29]. *In vitro* data suggests that synaptic transmission can result in productive infection of targets cells and result in high multiplicity of infection [41]. In order to explicitly include spatial dynamics of cell-to-cell transmission, we turn to a stochastic agent-based model. This includes both free virus and cell-to-cell transmission, and is adaptable to make either transmission process spatial or non-spatial. We consider a $\mathcal{N} \times \mathcal{N}$ two-dimensional grid, where each grid point can be empty, contain an uninfected cell, or contain an infected cell. Infected cells can contain any natural number of virus copies. For each time step we randomly make $\mathcal{N}^2$ updates to the grid

according to the following rules:

- empty grid points can become uninfected cells with probability λ;
- uninfected cells can die with probability d;
- infected cells can die with probability a, infect another cell by free virus transmission with probability β, or infect another cell by cell-to-cell transmission (with S copies of the virus) with probability γ. During the infection processes, a target spot is chosen randomly either from the entire grid or the local neighborhood. If that target spot contains a susceptible cell (uninfected or already infected), the infection event proceeds, otherwise it is aborted.

We assume that synaptic transmission can only occur to one of the eight nearest neighbors, while free virus transmission can occur to any cell on the grid. Basic simulations of this model can be seen in Supplemental figures S3 and S4.

It is straightforward to extend the agent-based model to include two virus strains that compete for the same target cell population (also see corresponding ODEs (5-6) of the Supplement, Section 1). In this setting, a cell can be infected by i copies of virus strain A and j copies of virus strain B. If a cell containing both virus strains is chosen for an infection event, the probability to transmit a given virus strain is proportional to the fraction of the strain among all viruses in the cell if the two strains are neutral with respect to each other. If the two strains have different replication rates, the fitness difference is implemented during the infection event, which can correspond to different rates of reverse transcription. That is, an infecting strain is again chosen randomly with a probability that is proportional to its fraction in the cell. A disadvantageous / advantageous mutant would then have a lower / higher probability to infect the chosen target cell upon infection. In this way, a strain's fitness is independent of whether or not it is contained within a coinfected cell. This method of modeling fitness is one choice among many, others are explored further in [27]. Additional assumptions could in principle be included here, such as complementation or inhibition among viruses within the same cell. Due to the complexity of the dynamics considered, however, our aim was to first study those in a simpler setting where such higher level interactions do not occur. Those more complex scenarios can be explored in future work, based on the detailed insights that are generated in the current paper.

In the neutral case, drift is observed with the eventual fixation of one of the virus strains. If the two virus strains have different fitness, the strain with the larger basic reproductive ratio [36] wins. Both of these cases can be seen in Supplemental figure S3.

1.2 Mutations and recombinations

We consider a virus population that can mutate at two different sites, denoted by a and b. Simulations are started with unmutated wild-type cells, ab. Single-mutant viruses (Ab or aB) can be generated during infection by point mutations, which occur with a probability μ per site. Each single-mutant can in turn mutate further to give rise to a double mutant AB. Note that a wild-type virus can directly mutate into a double mutant with a probability μ^2 if both sites mutate during the same reverse transcription event. The model also takes into account back-mutations, which again occur with a probability μ during an infection event. All the possible mutation events are illustrated in figure S1 of the Supplement.

Apart from mutations, however, a double mutant can also be generated through the recombination of different single-mutant viruses. This is implemented as follows. When viruses from a given source cell are chosen to infect a target cell, two virus genomes are randomly chosen with

a probability that is proportional to the fraction of their abundance in the cell. The first virus genome that is chosen is the template from which reverse transcription is initiated. If no recombination occurs, reverse transcription is assumed to proceed on this genome only. Recombination is assumed to occur with a probability ρ. In this case, the reverse-transcribed virus is assumed to be a recombinant, the identity of which depends on the two infecting genomes. Figure S2 of the Supplement list all recombination events that can occur.

There are two recombination processes in particular that are important: (i) $Ab + aB \rightarrow AB$ with probability $\rho/2$ (or ab with probability $\rho/2$), and (ii) $ab + AB \rightarrow Ab$ with probability $\rho/2$ or aB with probability $\rho/2$. These processes capture two roles of recombination that have been previously discussed in the literature [5]. Recombination between two single mutants can promote the generation of the double mutant, but recombination can also break up a double mutant upon recombination with the wild-type virus.

1.3 Simulations of the model and parameter values

We initialize the infection by randomly and uniformly spreading an equilibrium number of infected cells across the grid. These cells are singly infected with the wild type. We used a mutation rate of 3×10^{-5} [31] and a recombination rate $\rho = 0,\ 0.1, 0.2$, and 0.5. Most of the parameters of this system are unknown. The average life-span of productively infected cells is around 2 days[1] [39], and the basic reproductive ratio (R_0) of HIV (and SIV) has been estimated to be around 8 [40, 37]. In our simulations, the fitness of viruses varies, depending on whether the virus is wild-type, a one-hit mutant, or a two-hit mutant. Therefore, we chose parameters (provided in figure legends) such that the base-line $R_0 \sim 5$, which is in the correct order of magnitude. For advantageous mutants (single and double), the value of R_0 increases, depending on the assumptions about the fitness landscape. For disadvantageous mutants, the value of R_0 decreases, depending on the nature of the fitness landscape. R_0 calculations are given for the free virus transmission scenario (mass action) in section 1 of the supplement. For the spatial scenario (synaptic transmission), the expression for R_0 is currently not worked out, but for the same parameters is lower than for mass action. We assume that the uninfected cell death rate is half of the infected cell death rate, so that the average life-span of uninfected cells is around 4 days. The life span of susceptible T cells *in vivo* has been shown to be heterogeneous, with life-spans ranging from few days to several weeks, depending on the subpopulation under consideration [14].

In general, the multiplicity of infection in such models depends on virus load. For non-spatial, free virus transmission, the number of cells infected with i viruses correlates with the ith power of the singly infected cell population. In spatially structured models including synaptic transmission, the number of multiply infected cells correlates linearly with the number of singly infected cells. For the parameter values considered here, the average equilibrium multiplicities were as follows. In regimes where the basic reproductive ratio of the virus is around 8, the average multiplicity of infection in cells lies between 4-14, depending on how prevalent synaptic transmission is assumed to be (free virus transmission only leads to an average MOI of 4, while synaptic transmission only results in an average MOI of 14). Widely varying estimates for average infection multiplicities have been published [20, 18, 19, 43], and there is some uncertainty about that. While some of these papers suggest that the above quoted MOI range is too high, reference [43] showed that in a minority subset of T cells, up to 175 viruses were transmitted, likely due to synaptic infection processes. This might imply a relatively large number of integration events in such cells, even if many of the transmitted viruses fail. To investigate scenarios in which the average infection multiplicity is on the lower end (between 1-3, depending on viral transmission mode), we modified the model to track time since infection and assumed that the probability of superinfection declines over time due to

[1] Note that the death rate parameter used in our simulations corresponds to the time units of hours.

receptor down-modulation [11]. This is described in the Supplementary Materials (Section 4).

To investigate the relative contribution of free virus transmission (β) and cell-to-cell transmission (γ) we ran the model for different combinations of $\beta + \gamma = c$, where c is a fixed constant, ranging from purely synaptic to purely free virus transmission. The average outcome of the simulations were determined, including the average generation rate of double mutants, the average fraction of double mutants at a specific time point, and the time until the double mutant population grew to 90%.

2 Generation and spread dynamics of the double mutant

We will present all results for a range of transmission mode combinations, ranging from 100% synaptic transmission to 100% free virus transmission. In this section, however, we will mainly discuss under what fitness landscapes and assumptions recombination generally promotes the presence of double mutant populations, and when it works against them. The subsequent section will then discuss in more detail how these basic patterns are modulated by synaptic versus free virus transmission.

2.1 Fitness landscapes and epistasis

Our investigation will span a variety of fitness landscapes, including neutral, advantageous, and disadvantageous mutants. Let us assume that a mutation in site A or B results in an identical change in the fitness of the virus. Then, possible fitness landscapes can be separated into three groups for both advantageous and disadvantageous mutants [5]: negative epistasis, no epistasis, and positive epistasis, see figure 1(a) for examples of these.

Notice that each of the landscapes with advantageous mutants can be written as a triple of numbers,

$$\big((1-s),(1-s)^{\alpha},1\big), \tag{1}$$

which represent fitness values of the wild types, one hit mutants and double mutants respectively. Here $s > 0$ measures the amount of advantage, and α represents epistasis. We have $\alpha > 1/2$ for positive epistasis, $\alpha < 1/2$ for negative epistasis, and $\alpha = 1/2$ for no epistasis landscapes. Define the relative (log) fitness of the one-hit mutants compared to that of wild types, $\Delta_1 = \ln(1-s)^{\alpha} - \ln(1-s) = (1-\alpha)|\ln(1-s)|$, and the relative (log) fitness of the two-hit mutants compared to that of one-hit mutants, $\Delta_2 = \ln(1) - \ln(1-s)^{\alpha} = \alpha|\ln(1-s)|$. Note that the sum of the two coordinates, $\Delta_1 + \Delta_2 = |\ln(1-s)|$ represents the relative log fitness of the two-hit mutants compared to the wild types.

Similarly, each of the landscapes with disadvantageous mutants presented in figure 1(a) can be written as a triple of numbers,

$$\big(1,(1-s)^{\alpha},(1-s)\big), \tag{2}$$

where $s > 0$ measures the amount of disadvantage. The relative (log) fitness of the one-hit mutants compared to that of wild types, $\Delta_1 = \ln(1-s)^{\alpha} - \ln(1) = \alpha\ln(1-s)$. The relative (log) fitness of the two-hit mutants compared to that of one-hit mutants, $\Delta_2 = \ln(1-s) - \ln(1-s)^{\alpha} = (1-\alpha)\ln(1-s)$. Again, the sum of the two coordinates, $\Delta_1 + \Delta_2 = \ln(1-s)$, represents the relative log fitness of the two-hit mutants compared to the wild types.

2.2 Advantageous mutants

A reasonable measure of double mutant success is the time it takes for the double hit mutant to reach 90% of all infected cells. The following factors trade-off to determine whether recombination

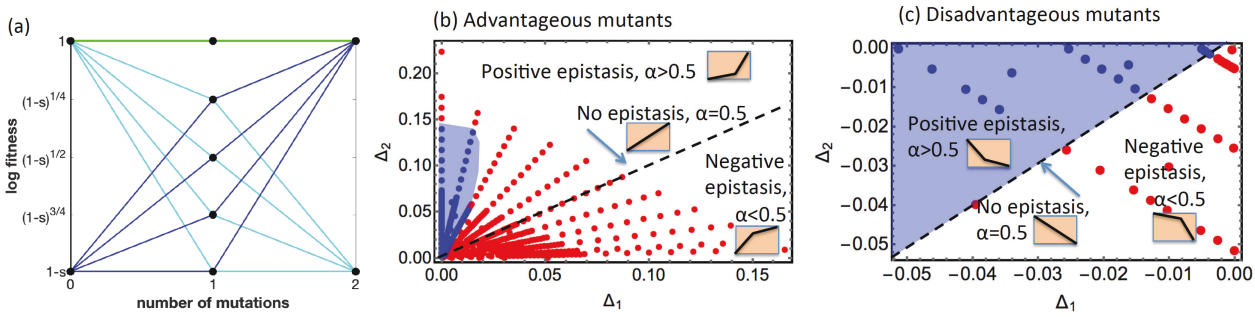

Figure 1: Summary of different scenarios. (a) Examples of fitness landscapes used in the simulations neutral (green), disadvantageous (cyan), advantageous (dark blue). Without epistasis the single-mutant fitness is given by $f = (1-s)^{1/2}$. For negative and positive epistasis examples in the figure, it is given by $(1-s)^{1/4}$ and $(1-s)^{3/4}$ respectively. For the extreme form of positive epistasis, single-mutant fitness is the same as that of wild types, $1-s$. (b-c) Role of recombination for different fitness landscapes. The horizontal axis is Δ_1 and the vertical axis is Δ_2, which are the relative log fitness values of single and double mutants, respectively. Each of the dots corresponds to a particular fitness landscape. (b) Advantageous mutants: Red dots correspond to runs in which recombination accelerated double hit mutant invasion to 90%, while blue dots indicate that recombination slowed down invasion. The boundary between the regions represents where there are no significant results one way or another. (c) Disadvantageous mutants: Red dots indicate that recombination increased the double mutant fraction at $T = 10^5$, while blue dots mean that recombination reduced the double mutant fraction. Blue shading marks the regions where recombination suppresses double hit mutants. The dashed black line corresponds to the cases of no epistasis ($\alpha = 0.5$) and separates the regions with positive epistasis ($\alpha > 0.5$) and negative epistasis ($\alpha < 0.5$) . For both (b) and (c), we fixed the probability of free-virus transmission at 40% ($\beta = 0.04$); the rest of the parameters are as in figure 2. The determination on whether recombination suppressed or enhanced double hit mutants was made by a statistical comparison of the averages over many runs, using the t test.

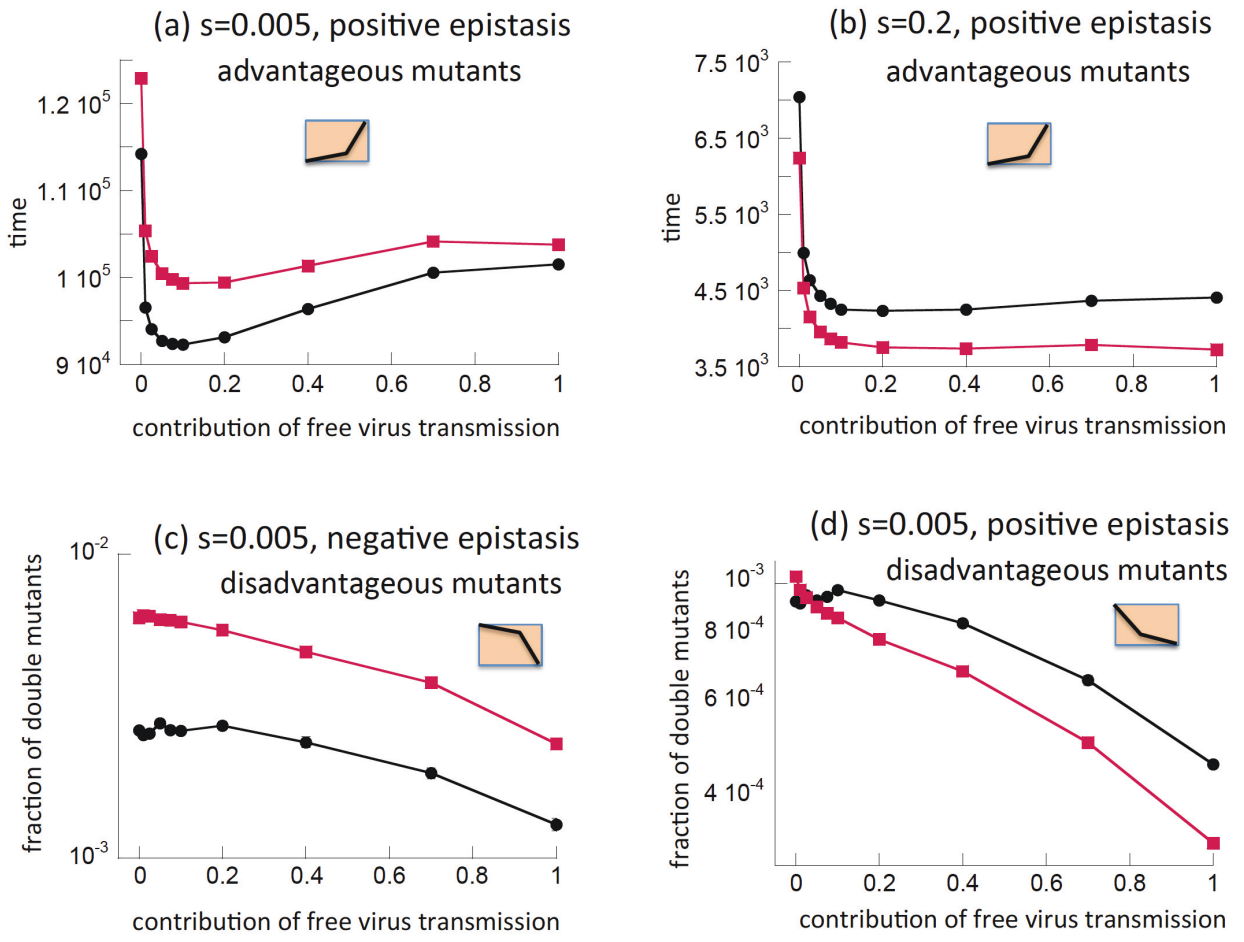

Figure 2: The role of recombination in (a,b) advantageous and (c,d) disadvantageous mutant dynamics; fitness landscapes are shown schematically in the insets. Red: with recombinations, and black: without recombination. (a-b) The time until the advantageous mutant reaches 90%, as a function of the fraction of free virus transmission. The means and standard errors are shown. For equivalent plots with standard deviations, see the Supplementary Materials Section 5.3. (a) $s = 0.005$, $\alpha = 0.75$. (b) $s = 0.2$, $\alpha = 0.75$. (c-d): The fraction of disadvantageous mutants at time $T = 10^5$, as a function of the fraction of free virus transmission. The means and standard errors are shown. (c) $s = 0.005$, $\alpha = 0.25$ (d) $s = 0.005$, $\alpha = 0.75$. The parameters are: $\beta + \gamma = 0.1$, $S = 3$, $\lambda = 1$, $d = 0.01$, $a = 0.02$, $\mathcal{N} = 100$, $\mu = 3 \times 10^{-5}$. All averages are based on at least 10^4 simulations.

boosts or suppresses double mutant spread: (i) Recombination between single mutants increases the rate at which double mutants are generated; (ii) recombination between double mutants and wild-type can break apart double mutants. (iii) the strength of selection of the double mutant defines how long the previous two factors are at play.

The net effect of recombination depends on the degree of the selective advantage, parameter s. For stronger advantages (larger values of s), recombination reduces the time to double mutant invasion (figure 2(b)). For lower selective advantages (lower s), however, recombination increases the time to double mutant invasion (figure 2(a)). The stronger the selective advantage, the quicker the double mutants spread at the expense of the wild-type, and then less likely it is that detrimental recombination events with the wild-type virus occur. This is illustrated with specific realizations of the stochastic dynamics in the Supplementary Section 3, figure S6.

The selective advantage threshold below which recombination slows double mutant invasion depends on the nature of the fitness landscape, in particular the value of α. This is summarized in figure 1(b). The horizontal axis is Δ_1 (fitness difference between single-mutant and wild-type) and the vertical axis is Δ_2 (fitness difference between double and single mutants). Each point in this coordinate system corresponds to a unique fitness landscape. The red color means that recombination events promote double mutant invasion, and blue means that they suppress this process. This picture has been composed by assuming 40% free virus transmission, and 60% synaptic transmission. Arrays of points radially fanning out of the origin correspond to landscapes with the same level of epistasis (the same value of α) but different selection strength (the closer to the origin, the lower s). We observe that for any level of epistasis, for sufficiently high fitness advantage, recombinations are advantageous for double hit mutants. As we decrease fitness s, however, there comes a point where recombinations no longer enhance double mutants but instead suppress them. In other words, any radial line will enter the blue region if it is sufficiently close to the origin. Recombinations can suppress the double mutant population significantly even for relatively large fitness advantages (large value of s) if α is relatively large and converges to one, i.e. for large positive epistasis (points close to the vertical axis in figure 1(b)). For lower values of α (weaker positive epistasis, no epistasis and negative epistasis), however, the transition happens for progressively smaller values of s. For large negative epistasis, the transition happens for very small values of s (for example, calculations show that for $\alpha = 0.25$, the blue region starts at about $s \approx 10^{-5}$, which is too small to see clearly in the figure and irrelevant for practical purposes, because such mutants are effectively neutral and take on average very long times to rise). The intuitive explanation for these observations is that lower values of α result in a more pronounced fitness advantage of single-hit mutants compared to wild-type virus. This in turn results in a faster exclusion of the wild-type virus population, and thus reduces the chances that recombinations break the double mutants. Hence, the parameter regime in which recombinations have a net negative effect on the double mutant population becomes more restrictive.

2.3 Disadvantageous mutants

A selective disadvantage leads to competitive exclusion in the absence of mutational processes. In the presence of mutational processes, disadvantageous mutants on average persist at an equilibrium level determined by the balance between mutation and selection. Hence, we determined the average fraction of double mutants at a time when this equilibrium has been reached, for different combinations of synaptic and free virus transmission (see Supplement Section 3.2 for details).

Recombination increases the double mutant population at the selection-mutation balance for negative epistasis (figure 2(c)), but tends to reduce it for positive epistasis if a sufficient amount of free virus transmission is assumed to occur (figure 2(d)). Similar results have been reported in the context of HIV drug resistance evolution [28]. If most virus transmission, however, occurs through

the synaptic route, figure 2(d) suggests that the opposite becomes true: Now, recombination can increase the mutant levels for positive epistasis as well. This will be explored in more detail below.

These trends are further illustrated in figure 1(c), assuming that a mixture of free virus and synaptic transmission occurs: As the parameter α is increased, the effect of recombination on the equilibirium level of double mutants changes from beneficial to detrimental. For the particular mixture of synaptic and free virus transmission chosen in this figure, recombination increases double mutant levels for negative epistasis (red region), and suppresses double mutant levels for positive epistasis (blue region). An increase in the parameter α results in a lower fitness of single mutants relative to the wild-type virus. This results in a higher prevalence of the wild-type virus, and thus in higher chances for the wild-type to recombine with and break apart the double mutant; see Supplement Section 3.3 for an ODE approximation of these results.

2.4 Neutral mutants

It follows from the above analysis that recombination delays the drift of neutral mutants towards dominance. Consider very weakly advantageous mutants in figure 1(b). We can see that the origin is contained in the blue region, that is, as the selective advantage $s \to 0$, we expect recombinations to delay the rise of double mutants.

For neutral mutants, however, the rise to dominance will take a very long time. Interestingly, different results are obtained if we look at the fraction of double mutants at an early time point T relative to when the double mutant strain has reached its average equilibrium. Figure 3(a) shows that recombination increases the fraction of double mutants at time T. This can be understood by considering the early vs long-term dynamics of neutral mutants. In the long-run, the populations will converge to a state where all four virus strains fluctuate around comparable fractions. This steady state is the same whether recombination occurs or not. The speed with which the double mutant rises towards this steady state, however, is influenced by the occurrence of recombination (figure 3(b,c)). Initially, the populations of single mutants are generated by mutations and rise by drift. In the absence of recombinations, double mutants are created and destroyed by mutations and also experience drift (panel (b)). In the presence of recombinations, however, double hit mutants initially enjoy positive selection due to relatively frequent recombination events between complimentary single hit mutants (which greatly outweigh the "breaking" recombination events of the double mutants with the wild type, due to the low levels of the former population). This can be seen in panel (c) of figure 3. Once the levels of double hit mutants increase, however, the "making" and "breaking" recombination events begin to balance each other and the dynamics return to neutral.

3 Mode of viral transmission and the effect of recombination on double mutant populations

The last section examined under what fitness landscapes recombination promotes or hinders the existence of double mutants. For advantageous and neutral mutants, these results remain robustly independent of the mode of virus transmission (Supplementary Section 5.1). For disadvantageous mutants, however, we noted that results can change if most virus transmission is assumed to be synaptic. Figure 2 showed that while for smaller values of α (negative epistasis, panel (c)), recombination lead to an increase in double mutant levels, for large values of α (positive epistasis, panel (d)), the opposite occurred and recombination reduced the double mutant levels. At the same time, however, figure 2(d) indicated that if most virus transmission occurs through the synaptic pathway, recombination remains helpful for the double mutant population even for positive epistasis. This is

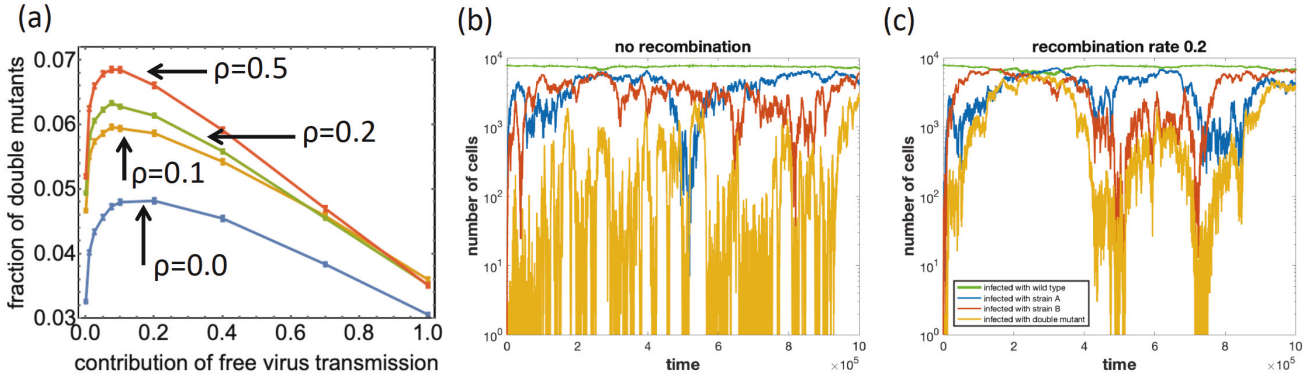

Figure 3: Neutral mutants. (a) The fraction of mutants after $T = 10^5$ steps. The horizontal axis is the fraction of free virus transmission. 4 values of ρ are presented from $\rho = 0$ (no recombinations) to $\rho = 0.5$ (maximal recombinations). The means of at least 40,000 runs at each location and standard errors are shown. (b,c) The dynamics of cell populations, typical time-series: (b) no recombinations, (c) with recombinations; we used $\beta = 0.04$ and $\gamma = 0.06$ (40% free virus transmission and 60% synaptic transmission). The other parameters are: $S = 3$, $\lambda = 1$, $d = 0.01$, $a = 0.02$, $\mathcal{N} = 100$, $\mu = 3 \times 10^{-5}$, $\rho = 0.2$.

explored in more detail in figure 4, which plots the equilibrium level of a disadvantageous mutant as a function of the parameter α for both extreme transmission modes: 100% free virus and 100% synaptic. If only free virus transmission occurs (panel (a)), recombination increases the double mutant fraction for $\alpha < 0.5$ (negative epistasis), while it decreases it for $\alpha > 0.5$ (positive epistasis). In contrast, if only synaptic transmission occurs (panel (b)), recombination always increases the number of double mutants, regardless of the value of α, although the double mutant levels in the presence and absence of recombination become practically indistinguishable for large values of α (strong positive epistasis). Supplemental figure S11 contains further simulations showing the robustness of these patterns for different levels of mutant disadvantage. Similar patterns hold for lower infection multiplicities (Section 4, Supplementary Materials). While for lower multiplicities, the equilibrium fraction of double mutants can still be slightly reduced by recombination for purely synaptic transmission, this reduction is much less than in the presence of only free virus transmission, thus confirming the protective effect of synaptic transmission even in the low multiplicity scenario. Therefore, if positive epistasis is present, as is suggested for drug resistance mutations in HIV [4], a prevalence of synaptic transmission can protect against the negative effects of recombination on the level at which drug-resistant mutations pre-exist before the start of treatment.

The intuitive explanation for the detrimental effect of recombination on the double mutant population at larger values of α was given in the previous section: For larger values of α, the fitness of single mutants relative to wild-type viruses becomes lower. This leads both to a slower rate of double mutant production, and to a higher prevalence of wild-type viruses that can recombine with the double mutant and break it. If most of virus transmission occurs through virological synapses, however, the spatially restricted virus spread that is assumed to occur with this transmission mode results in the generation of single and double mutant "clusters" or "islands". Single-mutant islands protect them from being outcompeted, resulting in larger numbers and thus a higher rate of double mutant generation. Double mutant islands isolate them from contact with wild-type virus, which prevents those detrimental recombination events from occurring. These dynamics are similar to the effect of "mutant islands" discussed in [22, 26].

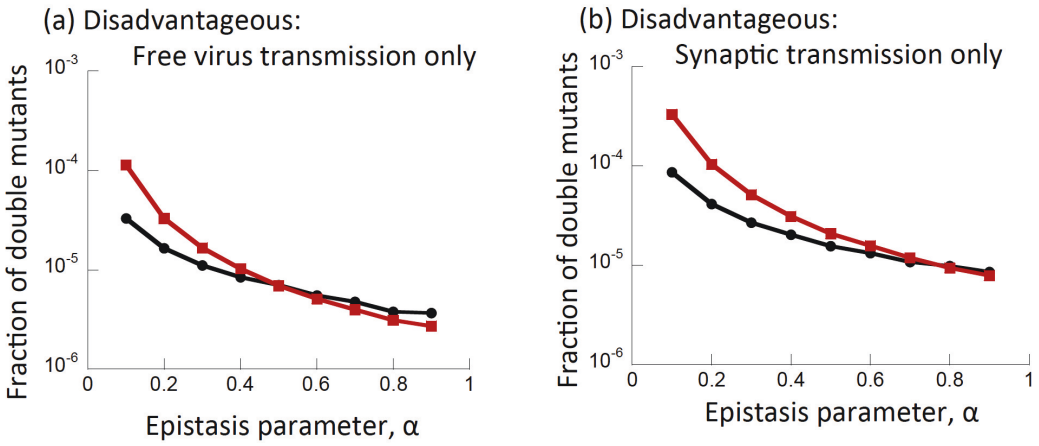

Figure 4: The role of recombinations under different transmission modes, for disadvantageous mutants. Shown is the temporal average of the fraction of double mutants at selection-mutation balance, as a function of that parameter α, defining the nature and extent of epistasis. Red denotes simulations with recombination and black without recombinations. (a) Free virus transmission only, (b) synaptic transmission only. $s = 0.05$, and other parameters are as in figure 2. Standard errors are too small to see. For equivalent plots with standard deviations, see the Supplementary Materials Section 5.3.

4 Mode of viral transmission and the rate of double mutant emergence

All simulations were performed for varying combinations of synaptic and free virus transmission, yet we have so far not discussed the effect of this itself on the emergence of the double mutant population. A number of factors trade off to determine what combination of synaptic and free virus transmission is optimal for the double mutant population. On the one hand, synaptic transmission results in the simultaneous transfer of multiple viruses from the source cell to the target cell, which increases the rate at which mutants are generated, and increases the rate of co-transmission of genetically different viruses, which in turn promotes the occurrence of recombination. On the other hand, if synaptic transmission is spatially restricted, as indicated by data [29], the rate at which the number of infected cells increases is slower under this mode of transmission, and it is less likely that genetically different strains come together in the same cell. For the different mutant types, the net effect is as follows:

Disadvantageous mutants: For disadvantageous mutants, more synaptic transmission tends to increase the equilibrium levels of double mutants at the selection-mutation balance (figure 2(c,d) and Supplemental figure S9(a,b) for the model with limited multiplicity). The main driving force responsible for the abundance of double mutants is production. This is maximized by synaptic transmission, because under this mechanism, there are more possibilities for mutations. Spread to higher levels is not an important force for disadvantageous mutants.

Advantageous mutants In the case of advantageous mutants, the rate of double mutant invasion tends to be increased by free virus transmission, and purely synaptic transmission results in the slowest rate of invasion (figure 2(a,b)). The reason is that in this scenario, the spread of the double mutant from low to high numbers is the driving process, and this is slower for synaptic transmission, which is assumed to be spatially restricted [29]. While increasing the contribution of free virus transmission generally speeds up mutant invasion, this trend can weaken or reverse for larger fractions of free virus transmission, which can result in a shallow optimum, see figure 2(a,b)

and Supplemental figure S9(c-e) for the model with limited multiplicity. The reason is that in the absence of significant synaptic transmission, fewer overall infection, and hence reverse transcription, events occur, which delays mutant production.

Neutral mutants: In the neutral case, and also for very weakly advantageous and disadvantageous mutants, a mixture of both free virus and cell-to-cell transmission maximizes the fraction of cells infected with the double mutant (figure 3(a) and Supplemental figure S9(f) for the model with limited multiplicity). This result is similar to what was observed in Section 2 of the Supplement, where the generation time of double hit mutants was studied. Here we observe that this holds even in the absence of recombination, and is more pronounced. The reason is that while more synaptic transmission results in the simultaneous transfer of multiple viruses, and hence in more chances to mutate, it also slows down the increase of the infected cell population due to the assumed spatial restriction. In this scenario, both production and spread play important roles.

5 Discussion and Conclusion

We aimed to comprehensively analyze the effect of recombination on double mutant evolution in the context of HIV, depending on the details of fitness landscapes and the assumptions about the mode of viral spread (relative importance of synaptic versus free virus transmission). This is different from previous approaches, which focused more specifically on the evolution of drug resistance in HIV in the context of only free virus transmission, and concentrated on specific fitness landscapes characterized by positive or negative epistasis. Our approach characterized the fitness landscape by the parameter α, which could be continuously varied from 0 to 1, thus capturing all fitness landscapes ranging from negative to positive epistasis for advantageous and disadvantageous mutants. The constraint in our fitness landscapes was that the two different single-hit mutants were assumed to have identical fitness. Another constraint of our analysis was that certain parameters of the system were kept constant throughout this analysis, such as the production rate and death rate of target cells or the death rate of infected cells, due to the complexity of the scenarios considered. We did perform selective simulations assuming different values for these parameters (see Section 5.4 and Table 1 of the Supplement) and did not find a qualitative change in the results, but an exhaustive analysis of the entire parameter space was not feasible. A tree showing an overview of the main results can be seen in Figure 5.

The opposing effect of recombination to make and break double mutants played out as follows in the model analyzed here: For advantageous mutants, recombination largely accelerates double mutant invasion except for cases of very strong positive epistasis with an intermediate fitness advantage of the mutants, or in cases where the fitness advantage becomes relatively low. The mode of viral spread does not modulate these patterns. If the mutants are disadvantageous, however, the mode of virus spread can significantly influence the effect of recombination on the equilibrium level of double mutants at selection-mutation balance. If the contribution of free virus transmission to virus spread lies above a threshold, recombination increases the double mutant population for negative epistasis, but decreases it for positive epistasis. If the dominant mode of virus spread is synaptic transmission, however, the negative effect of recombination for positive epistasis is greatly reduced, indicating a protective effect on the persistence of disadvantageous double mutants. In fact, for higher multiplicities, recombination increases double mutant levels even for positive epistasis if synaptic transmission is the dominant mode of virus spread. Finally, for neutral mutants, we observed that recombination always delays the rise of double mutants to dominance, but at the same time increases double mutant fractions measured at a relatively early time points in the dynamics. Interestingly, neutral double mutant dynamics in the presence of recombination are characterized by an "advantageous" initial growth phase before converging to neutral drift, which explains the positive effect of recombination on early double mutant fractions.

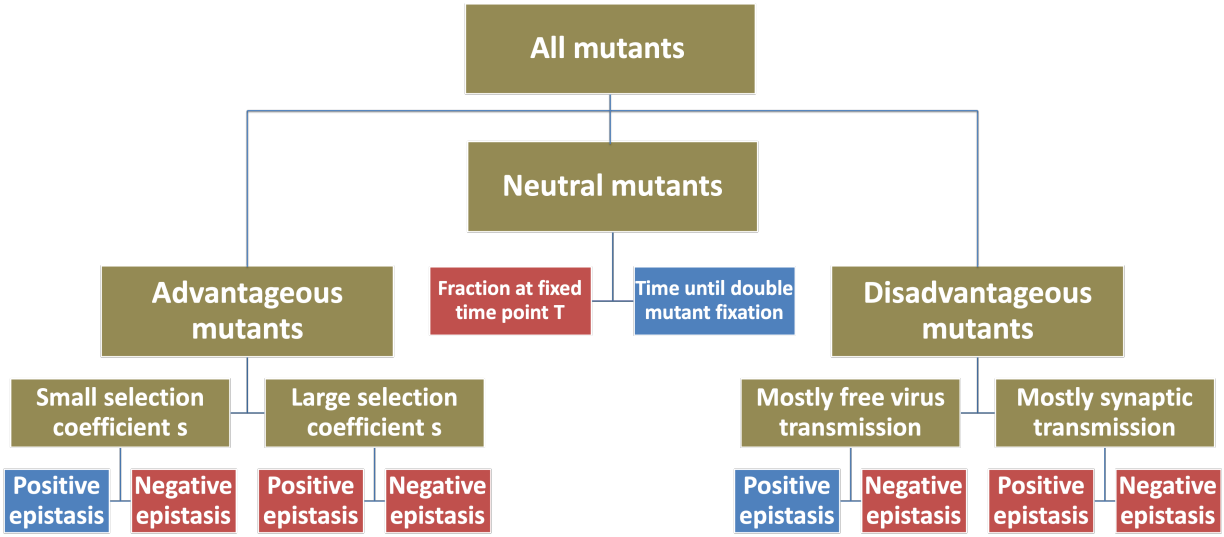

Figure 5: An overview of the main results. Here red boxes correspond to situations in which recombination accelerated double mutant evolution, whereas blue boxes indicate that recombination slowed down double mutant evolution.

These findings have implications for the pre-existence of multi-drug resistant HIV mutants before the start of therapy. In the absence of treatment, resistant mutants typically carry a fitness cost. Moreover, evidence for positive epistasis has been observed in HIV resistance evolution [4]. Therefore, a relatively high rate of synaptic transmission could significantly increase the chances that multi-drug resistant virus mutants are present at selection-mutation balance before treatment is initiated.

The way in which the mode of virus spread was observed to influence the rate of double mutant emergence was driven by two opposing effects: synaptic virus transmission increases double mutant production in our model, but slows down double mutant spread due to the experimentally supported assumption that synaptic transmission is associated with spatially clustered dynamics [29]. For disadvantageous mutants, production is the main driving force, and hence purely synaptic transmission results in highest mutant levels. For advantageous mutants, double mutant spread is a crucial factor, and hence, free virus transmission tends to speed up mutant invasion in our model. For neutral mutants, both production and spread are similarly important, and hence, there is an optimal combination of free virus and synaptic transmission that maximizes double mutant fractions.

This again reinforces the notion that synaptic transmission promotes the pre-existence of drug resistance mutants before therapy, since such mutants tend to be disadvantageous. More generally, our results suggest that synaptic transmission increases the persistence of disadvantageous mutants at selection-mutation balance, which could later become advantageous due to changes in selection pressures. At the same time, however, synaptic transmission is predicted to slow down the invasion of mutants that have escaped two (or more) immune response specificities (CD8 T cell or B cell responses), since escape mutations are advantageous. The model suggests that the invasion of such mutants is promoted by free virus transmission. Escape from two immune cell clones with different specificities is likely characterized by positive epistasis. If a virus population is controlled by two immune cell clones with different specificities, escape from one of them probably leads to an incre-

mental fitness increase, while escape from both clones can result in a significant loss of control. In this scenario, the model further suggests that recombination promotes the rise of double immune escape mutants if escape leads to a sufficiently large fitness advantage, which is likely to be true. Finally, the presence of neutral genetic diversity is predicted to be maximized by an optimal balance between synaptic and free virus transmission. This discussion emphasizes that the mode of virus spread does not have a universally positive or negative effect on mutant persistence or emergence, and that the effect depends on the exact nature of the mutants under consideration.

There is some controversy in the literature about the average multiplicity of infected cells *in vivo*. While some papers reported significant levels of multiple infection, especially in tissue compartments [20, 43], other publications found an infection multiplicity close to one, both in the blood and tissues [18, 19]. Reasons for the discrepancy could be the methodology that was used to measure multiplicity, and also the T cell subsets that were taken into account during this analysis. In the light of data that document an important contribution of recombination to the *in vivo* evolution of HIV [30, 20, 34, 33], it is likely that a sufficient amount of multiple infection occurs. An important role of multiple infection is further suggested by studies that document a very efficient infection process during synaptic cell-to-cell transmission, resulting in the simultaneous transfer of multiple viruses from the source cell to the target cell [7, 17, 42]. Further, the frequent co-transmission of different virus strains was observed both *in vitro* and *in vivo* [8, 29]. An important point in our analysis was that a model with reduced infection multiplicity due a declining ability to super-infect over time resulted in similar insights.

Another crucial assumption of our model was that synaptic cell-to-cell transmission was characterized by spatially restricted virus spread. While imaging studies have shown an ability of immune cells to move about within tissues [13], our work on humanized mice demonstrated that virus spread in the presence of synaptic, cell-to-cell transmission, was characterized by the spatial clustering of infected cells [29], which supports the assumption we made. If it were assumed that synaptic transmission follows mass action law, then several results would change, since synaptic transmission would no longer give rise to slower virus spread than free virus transmission. While there is evidence that HIV infected cells are motile, we assume that they are static within the context of the agent-based model and that mixing effects occur through non-spatial transmission [35]. A certain amount of cell migration could be incorporated into the model, and this would be an interesting future extension of the current work. While we have investigated the effect of spatially restricted virus transmission in the context of a 2D model (which might best represent in vitro conditions), the geometry of cell arrangements in the lymphatic tissues is more complex and in fact not documented in detail. A 3-dimensional version of this model could be a next step when increasing complexity, but a biologically more realistic computational description will require more detailed data to be collected that characterize the exact spatial arrangement of T cells and their migration patterns.

The relative contribution of synaptic and free virus transmission to virus spread *in vivo* is still not well-understood. *In vitro* experiments have estimated that the two transmission modes contribute approximately equally to virus spread [23], but conditions *in vivo* are likely significantly different, and this could have a large impact on these dynamics. Our results indicate that both free virus and synaptic transmission have important and different effects on double mutant populations, depending on the nature of the mutants. Free virus transmission promotes the invasion of advantageous double mutants, while synaptic transmission promotes the existence of disadvantageous double mutants at selection-mutation balance. Further, we observed synaptic transmission to protect against negative effects of recombination for disadvantageous double mutants characterized by positive epistasis. These selective forces likely shape the balance between synaptic and free virus transmission towards which HIV has evolved.

An important next step will be to address some of the insights obtained from our modeling with data. Because our models examine the role of synaptic and free virus transmission for double mutant evolution, and investigate the impact of recombination on these dynamics, this requires a system that can be easily manipulated in these respects. We have previously analyzed HIV dynamics *in vitro* under static conditions, where both free virus and synaptic transmission occurs, as well as under gentle shaking conditions, where synaptic transmission is largely disrupted and most virus spread occurs via the release of free viruses [23]. Viruses that are labeled with two different fluorescent reporter genes, and upon recombination give rise to a third and distinct fluorescent color can be grown under these conditions [30]. This will allow us to experimentally parse the effect of different transmission modes on double mutant evolution and on the rate of recombination, and to relate experimental results to modeling predictions that are presented here. This is subject to ongoing work.

Acknowledgements

This work was supported by NSF grant DMS 1662146 /1662096.

Funding statement

This work was supported by NSF grant DMS 1662146 /1662096.

Author contributions

Jesse Kreger developed the computational models, analyzed them, ran computer simulations, and wrote the paper. Natalia Komarova developed the computational models, analyzed them, and wrote the paper. Dominik Wodarz developed the computational models, ran computer simulations, and wrote the paper.

Data accessibility

Agent-based model code is included in the supplementary materials.

References

[1] Luis M Agosto, Pradeep D Uchil, and Walther Mothes. HIV cell-to-cell transmission: effects on pathogenesis and antiretroviral therapy. *Trends in microbiology*, 23(5):289–295, 2015.

[2] Christian L Althaus and Sebastian Bonhoeffer. Stochastic interplay between mutation and recombination during the acquisition of drug resistance mutations in human immunodeficiency virus type 1. *Journal of virology*, 79(21):13572–13578, 2005.

[3] Ani Asatryan, Dominik Wodarz, and Natalia L Komarova. New virus dynamics in the presence of multiple infection. *Journal of theoretical biology*, 377:98–109, 2015.

[4] Sebastian Bonhoeffer, Colombe Chappey, Neil T Parkin, Jeanette M Whitcomb, and Christos J Petropoulos. Evidence for positive epistasis in HIV-1. *Science*, 306(5701):1547–1550, 2004.

[5] Michael T. Bretscher, Christian L. Althaus, Viktor Müller, and Sebastian Bonhoeffer. Recombination in HIV and the evolution of drug resistance: for better or for worse? *Bioessays*, 26.2:180–188, 2004.

[6] Antonio Carvajal-Rodriguez, Keith A. Crandall, and David Posada. Recombination favors the evolution of drug resistance in HIV-1 during antiretroviral therapy. *Infection, genetics and evolution*, 7(4):476–483, 2007.

[7] Ping Chen, Wolfgang Hübner, Matthew A Spinelli, and Benjamin K Chen. Predominant mode of human immunodeficiency virus transfer between T cells is mediated by sustained Env-dependent neutralization-resistant virological synapses. *Journal of virology*, 81(22):12582–12595, 2007.

[8] Armando Del Portillo, Joseph Tripodi, Vesna Najfeld, Dominik Wodarz, David N Levy, and Benjamin K Chen. Multiploid inheritance of HIV-1 during cell-to-cell infection. *Journal of virology*, pages JVI–00231, 2011.

[9] DS Dimitrov, RL Willey, H Sato, L-Ji Chang, R Blumenthal, and MA Martin. Quantitation of human immunodeficiency virus type 1 infection kinetics. *Journal of virology*, 67(4):2182–2190, 1993.

[10] Narendra M Dixit and Alan S Perelson. Multiplicity of human immunodeficiency virus infections in lymphoid tissue. *Journal of virology*, 78(16):8942–8945, 2004.

[11] Narendra M Dixit and Alan S Perelson. HIV dynamics with multiple infections of target cells. *Proceedings of the National Academy of Sciences*, 102(23):8198–8203, 2005.

[12] Christophe Fraser. Hiv recombination: what is the impact on antiretroviral therapy? *Journal of the Royal Society, Interface*, 2(5):489–503, 2005.

[13] Ronald N Germain, Ellen A Robey, and Michael D Cahalan. A decade of imaging cellular motility and interaction dynamics in the immune system. *Science*, 336(6089):1676–1681, 2012.

[14] Graeme Gossel, Thea Hogan, Daniel Cownden, Benedict Seddon, and Andrew J Yates. Memory cd4 t cell subsets are kinetically heterogeneous and replenished from naive t cells at high levels. *Elife*, 6:e23013, 2017.

[15] Vanessa M Hirsch. Evolution of the fittest ends in tragedy. *Nature medicine*, 5(5):488, 1999.

[16] David D Ho, Avidan U Neumann, Alan S Perelson, Wen Chen, John M Leonard, and Martin Markowitz. Rapid turnover of plasma virions and CD4 lymphocytes in HIV-1 infection. *Nature*, 373(6510):123, 1995.

[17] Wolfgang Hübner, Gregory P McNerney, Ping Chen, Benjamin M Dale, Ronald E Gordon, Frank YS Chuang, Xiao-Dong Li, David M Asmuth, Thomas Huser, and Benjamin K Chen. Quantitative 3D video microscopy of HIV transfer across T cell virological synapses. *Science*, 323(5922):1743–1747, 2009.

[18] Lina Josefsson, Martin S King, Barbro Makitalo, Johan Brännström, Wei Shao, Frank Maldarelli, Mary F Kearney, Wei-Shau Hu, Jianbo Chen, Hans Gaines, et al. Majority of CD4+ t cells from peripheral blood of HIV-1–infected individuals contain only one HIV DNA molecule. *Proceedings of the National Academy of Sciences*, 108(27):11199–11204, 2011.

[19] Lina Josefsson, Sarah Palmer, Nuno R Faria, Philippe Lemey, Joseph Casazza, David Ambrozak, Mary Kearney, Wei Shao, Shyamasundaran Kottilil, Michael Sneller, et al. Single cell analysis of lymph node tissue from HIV-1 infected patients reveals that the majority of CD4+ T-cells contain one HIV-1 DNA molecule. *PLoS pathogens*, 9(6):e1003432, 2013.

[20] Andreas Jung, Reinhard Maier, Jean-Pierre Vartanian, Gennady Bocharov, Volker Jung, Ulrike Fischer, Eckart Meese, Simon Wain-Hobson, and Andreas Meyerhans. Recombination: Multiply infected spleen cells in HIV patients. *Nature*, 418(6894):144, 2002.

[21] Jason T Kimata, LaRene Kuller, David B Anderson, Peter Dailey, and Julie Overbaugh. Emerging cytopathic and antigenic simian immunodeficiency virus variants influence AIDS progression. *Nature medicine*, 5(5):535, 1999.

[22] Natalia L Komarova. Loss-and gain-of-function mutations in cancer: mass-action, spatial and hierarchical models. *Journal of Statistical Physics*, 128(1-2):413–446, 2007.

[23] Natalia L Komarova, Daniela Anghelina, Igor Voznesensky, Benjamin Trinité, David N Levy, and Dominik Wodarz. Relative contribution of free-virus and synaptic transmission to the spread of HIV-1 through target cell populations. *Biology letters*, 9(1):20121049, 2013.

[24] Natalia L Komarova, David N Levy, and Dominik Wodarz. Effect of synaptic transmission on viral fitness in HIV infection. *PloS one*, 7(11):e48361, 2012.

[25] Natalia L Komarova, David N Levy, and Dominik Wodarz. Synaptic transmission and the susceptibility of HIV infection to anti-viral drugs. *Scientific reports*, 3:2103, 2013.

[26] Natalia L Komarova, Leili Shahriyari, and Dominik Wodarz. Complex role of space in the crossing of fitness valleys by asexual populations. *Journal of The Royal Society Interface*, 11(95):20140014, 2014.

[27] Natalia L Komarova and Dominik Wodarz. Virus dynamics in the presence of synaptic transmission. *Mathematical biosciences*, 242(2):161–171, 2013.

[28] Roger D Kouyos, David Fouchet, and Sebastian Bonhoeffer. Recombination and drug resistance in HIV: population dynamics and stochasticity. *Epidemics*, 1(1):58–69, 2009.

[29] Kenneth M Law, Natalia L Komarova, Alice W Yewdall, Rebecca K Lee, Olga L Herrera, Dominik Wodarz, and Benjamin K Chen. In vivo HIV-1 cell-to-cell transmission promotes multicopy micro-compartmentalized infection. *Cell reports*, 15(12):2771–2783, 2016.

[30] David N Levy, Grace M Aldrovandi, Olaf Kutsch, and George M Shaw. Dynamics of HIV-1 recombination in its natural target cells. *Proceedings of the National Academy of Sciences*, 101(12):4204–4209, 2004.

[31] Louis M Mansky and Howard M Temin. Lower in vivo mutation rate of human immunodeficiency virus type 1 than that predicted from the fidelity of purified reverse transcriptase. *Journal of virology*, 69(8):5087–5094, 1995.

[32] Meriet Mikhail, Bin Wang, Philippe Lemey, Brenda Beckthold, Anne-Mieke Vandamme, M John Gill, and Nitin K Saksena. Role of viral evolutionary rate in HIV-1 disease progression in a linked cohort. *Retrovirology*, 2(1):41, 2005.

[33] Rafal Mostowy, Roger D Kouyos, David Fouchet, and Sebastian Bonhoeffer. The role of recombination for the coevolutionary dynamics of HIV and the immune response. *PloS one*, 6(2):e16052, 2011.

[34] Laure Moutouh, Jacques Corbeil, and Douglas D Richman. Recombination leads to the rapid emergence of HIV-1 dually resistant mutants under selective drug pressure. *Proceedings of the National Academy of Sciences*, 93(12):6106–6111, 1996.

[35] Thomas T Murooka, Maud Deruaz, Francesco Marangoni, Vladimir D Vrbanac, Edward Seung, Ulrich H von Andrian, Andrew M Tager, Andrew D Luster, and Thorsten R Mempel. Hiv-infected t cells are migratory vehicles for viral dissemination. *Nature*, 490(7419):283–287, 2012.

[36] Martin Nowak and Robert M May. *Virus dynamics: mathematical principles of immunology and virology*. Oxford university press, 2000.

[37] Martin A Nowak, Alun L Lloyd, Gabriela M Vasquez, Theresa A Wiltrout, Linda M Wahl, Norbert Bischofberger, Jon Williams, Audrey Kinter, Anthony S Fauci, Vanessa M Hirsch, et al. Viral dynamics of primary viremia and antiretroviral therapy in simian immunodeficiency virus infection. *Journal of virology*, 71(10):7518–7525, 1997.

[38] Alan S Perelson. Modelling viral and immune system dynamics. *Nature Reviews Immunology*, 2(1):28, 2002.

[39] Alan S Perelson, Avidan U Neumann, Martin Markowitz, John M Leonard, and David D Ho. Hiv-1 dynamics in vivo: virion clearance rate, infected cell life-span, and viral generation time. *Science*, 271(5255):1582–1586, 1996.

[40] Ruy M Ribeiro, Li Qin, Leslie L Chavez, Dongfeng Li, Steven G Self, and Alan S Perelson. Estimation of the initial viral growth rate and basic reproductive number during acute HIV-1 infection. *Journal of virology*, 84(12):6096–6102, 2010.

[41] Rebecca A. Russell, Nicola Martin, Ivonne Mitar, Emma Jones, and Quentin J. Sattentau. Multiple proviral integration events after virological synapse-mediated hiv-1 spread. *Virology*, 443:443, 2013.

[42] Quentin Sattentau. Avoiding the void: cell-to-cell spread of human viruses. *Nature Reviews Microbiology*, 6(11):815, 2008.

[43] Alex Sigal, Jocelyn T Kim, Alejandro B Balazs, Erez Dekel, Avi Mayo, Ron Milo, and David Baltimore. Cell-to-cell spread of HIV permits ongoing replication despite antiretroviral therapy. *Nature*, 477(7362):95, 2011.

[44] Xiping Wei, Sajal K Ghosh, Maria E Taylor, Victoria A Johnson, Emilio A Emini, Paul Deutsch, Jeffrey D Lifson, Sebastian Bonhoeffer, Martin A Nowak, Beatrice H Hahn, et al. Viral dynamics in human immunodeficiency virus type 1 infection. *Nature*, 373(6510):117, 1995.

Supplementary Information

Effect of synaptic cell-to-cell transmission and recombination on the evolution of double mutants in HIV

Journal of the Royal Society Interface

Jesse Kreger[a], Natalia L. Komarova[a] and Dominik Wodarz[b,a]

a) Department of Mathematics, University of California Irvine, Irvine CA 92697

b) Department of Population Health and Disease Prevention Program in Public Health
Susan and Henry Samueli College of Health Sciences, University of California, Irvine CA 92697

Contents

1 Deterministic and stochastic modeling of synaptic and free virus transmission

1.1 Deterministic modeling: a review

Here, we review a previously published mathematical modeling framework to study the role of synaptic and free virus transmission in HIV dynamics [5, 3, 4]. This modeling approach is based on ordinary differential equations, which means that perfect mixing of populations occurs with both transmission modes, i.e. synaptic transmission is not spatially restricted. This is a severely limiting factor, however the ODE model also provides a framework that allows for mathematical analysis that is not possible with only the agent-based model. Let $x_i(t)$ be the population of cells infected with i copies of the virus at time t. Let γ_j^m be the parameter characterizing the rate at which cells infected with m viruses transmit j viruses per synapse, and let β represent the rate of free virus transmission. Let N be the maximum number of copies of the virus that a single cell can contain, known as the maximum infection multiplicity. No such maximum is needed in the agent-based

model, but here it simplifies solving the ODE model. The model equations with both free virus and synaptic transmission pathways are

$$\dot{x}_0 = \lambda - dx_0 - \beta x_0 \sum_{m=1}^{N} x_m - \sum_{m=1}^{N} x_m \sum_{j=1}^{N} \gamma_j^m x_0, \tag{1}$$

$$\dot{x}_i = \beta(x_{i-1} - x_i) \sum_{m=1}^{N} x_m + \sum_{m=1}^{N} x_m \Big(\sum_{j=1}^{i} \gamma_j^m x_{i-j} - x_i \sum_{j=1}^{N-i} \gamma_j^m \Big) - a x_i, \tag{2}$$

where λ is the constant production rate of uninfected target cells, d is the death rate of uninfected cells, and a is the death rate of infected cells. Note that in contrast to the agent-based model, the present model assumes that both free virus and synaptic transmission are non-spatial processes. Further, this model assumes that kinetic parameters are independent of infection multiplicity, because there is currently no evidence to the contrary.

Let us denote

$$\gamma = \sum_{m=1}^{N} \sum_{j=1}^{N} \gamma_j^m,$$

as the total rate of synaptic transmission. The model given by equations (1-2) is characterized by two outcomes / equilibria. The disease-free equilibrium is given by

$$x_0 = \frac{\lambda}{d}, \quad x_i = 0 \text{ for } 1 \leq i \leq N. \tag{3}$$

Virus persistence is described by the following equilibrium expressions:

$$x_0 = \frac{a}{\beta + \gamma}, \quad z = \frac{\lambda}{a} - \frac{d}{\beta + \gamma}, \tag{4}$$

where z denotes the sum of all infected cell sub-types. Additionally, one can calculate the steady state value for each individual infected population, see [5] for details.

An important measure in virus dynamics is the basic reproductive ratio of the virus, R_0, denoting the average number of newly infected cells produced by a single infected cell when placed into a pool of susceptible cells [8, 9]. In a deterministic model, if $R_0 > 1$, the virus successfully establishes an infection, and if $R_0 < 1$, virus extinction occurs. For the model written down here, the basic reproductive ratio of the virus is given by $R_0 = \frac{(\beta+\gamma)\lambda}{ad}$. Setting $\gamma = 0$, we reproduce the expression for R_0 derived from the basic model of virus dynamics in the absence of multiple infection and synaptic transmission [8, 9]. The reason for this is that kinetic parameters, such as the rate of virus production or the rate of virus-induced cell death, are assumed to be independent of infection multiplicity.

As done in [5], this model can be extended to include competition between two or more virus strains. Let $x_{ij}(t)$ be the population of cells infected with i copies of virus strain A and j copies of virus strain B at time t. Let γ_{qp}^{mk} be the probability for a cell infected with m copies of virus strain A and k copies of virus strain B to transmit q copies of virus strain A and p copies of virus strain

B. The model equations for competition between two strains are

$$\dot{x}_{00} = \lambda - dx_{00} - \beta x_{00} \sum_{m=0}^{N} \sum_{\substack{k=0 \\ m+k>0}}^{N-m} x_{mk} - x_{00} \sum_{m=0}^{N} \sum_{\substack{k=0 \\ m+k>0}}^{N-m} x_{mk} \sum_{q=0}^{N} \sum_{\substack{p=0 \\ p+q>0}}^{N-q} \gamma_{qp}^{mk}, \tag{5}$$

$$\begin{aligned} \dot{x}_{ij} &= \beta\Big(\frac{m}{m+k} x_{i-1,j} + \frac{k}{m+k} x_{i,j-1} - x_{ij}\Big) \sum_{m=0}^{N} \sum_{\substack{k=0 \\ m+k>0}}^{N-m} x_{mk} \\ &+ \sum_{m=0}^{N} \sum_{\substack{k=0 \\ m+k>0}}^{N-m} x_{mk} \Big(\sum_{q=0}^{i} \sum_{\substack{p=0 \\ p+q>0}}^{j} x_{i-q,j-p} \gamma_{qp}^{mk} - x_{ij} \sum_{q=0}^{N-i} \sum_{\substack{p=0 \\ p+q>0}}^{N-i-j-q} \gamma_{pq}^{mk} \Big) - a x_{ij}. \end{aligned} \tag{6}$$

In equation (6), we assume $i+j > 0$ and $i+j \leq N$. We also assume for all of the double summations that the two indices are not zero simultaneously. These equations can be extended naturally to include competition between any number of additional strains. As shown in [5], the outcome of this competition depends on the relative value of R_0 of the two virus strains. If the values of R_0 are identical, the strains are neutral with respect to each other, and an infinite number of equilibria exists, depending on the initial conditions. If the two strains have different values of R_0, then the strain with the higher R_0 wins and excludes the other strain.

1.2 A model with density-dependent target cell production

In order to match the standard ordinary differential equation model to our agent-based model, we need to employ a scaling of the rate parameters, as well as a density-dependent production term of target cells. This is because the agent-based model describes the system on a finite $\mathcal{N}$ by $\mathcal{N}$ grid. The model equations with the appropriate scalings are

$$\dot{x}_0 = \lambda\Big(\mathcal{N}^2 - x_0 - \sum_{m=1}^{N} x_m\Big) - dx_0 - \frac{\beta}{\mathcal{N}^2} x_0 \sum_{m=1}^{N} x_m - \sum_{m=1}^{N} x_m \sum_{j=1}^{N} \frac{\gamma_j^m}{\mathcal{N}^2} x_0, \tag{7}$$

$$\dot{x}_i = \frac{\beta}{\mathcal{N}^2}(x_{i-1} - x_i) \sum_{m=1}^{N} x_m + \sum_{m=1}^{N} x_m \Big(\sum_{j=1}^{i} \frac{\gamma_j^m}{\mathcal{N}^2} x_{i-j} - x_i \sum_{j=1}^{N-i} \frac{\gamma_j^m}{\mathcal{N}^2} \Big) - a x_i. \tag{8}$$

The adjustments of λ to $\lambda(\mathcal{N}^2 - x_0 - \sum_{m=1}^{N} x_m)$ and γ_j^m to $\frac{\gamma_j^m}{\mathcal{N}^2}$ need to be made from the standard ODE model to match the agent-based model. For instance, in the standard model λ represents the constant production rate of uninfected cells, however in the agent-based model λ represents the probability that a randomly chosen empty grid point becomes an uninfected cell, as we do not produce uninfected cells from anywhere else.

Here, we chose to work with the assumptions underlying the agent-based model, i.e. assuming that production of cells depends on cell concentration. Complex regulatory systems have been described for the hematopoietic system [11], so we consider this a biologically reasonable assumption. At the same time, we point out that there is uncertainty about the laws of target cell production, and more data are required to couple such assumptions more closely to reality.

This adjusted model is characterized by a similar solution structure and a similar bifurcation behavior as the basic model (1-2), but the expressions become somewhat different. For example, for model (7-8), we have $R_0 = \frac{(\beta+\gamma)\lambda}{a(\lambda+d)}$, and the steady state value corresponding to equation (4) becomes $z = \frac{\mathcal{N}^2((\beta+\gamma)\lambda - \lambda a - da)}{(\beta+\gamma)(\lambda+a)}$.

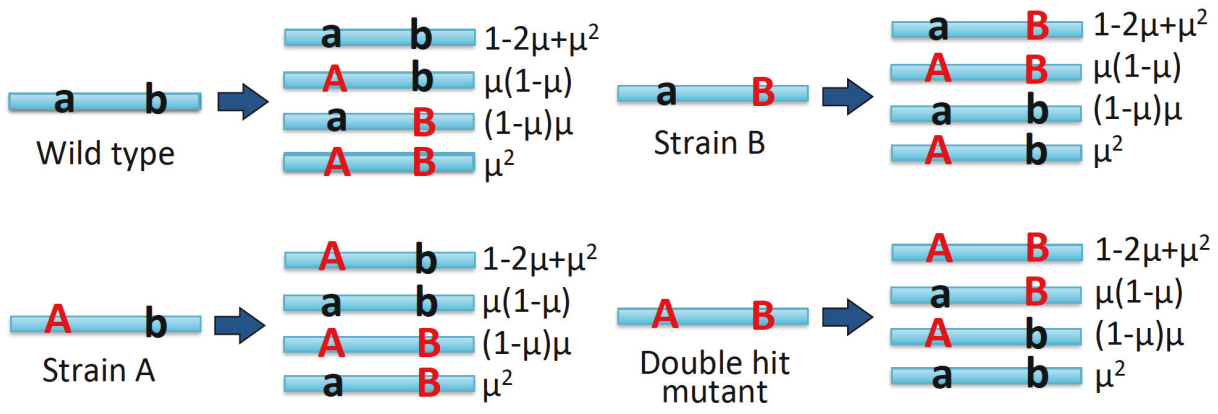

Figure S1: All mutation processes possibilities between the types, together with their probabilities.

1.3 Modeling mutations and recombinations

Figure S1 presents all the (forward and backward) mutation processes that can occur between the four types. Figure S2 presents all possible recombination events that can happen in the presence of two types of mutations. Only two events result in types different from either of the recombining types: the creation of a double hit mutant when mutant A recombines with mutant B, and the destruction of a double hit mutant (making it into a single mutant) when it recombines with the wild type virus.

1.4 Spatial stochastic simulations

Figure S3 shows a comparison of the stochastic, agent based model with the deterministic ODE model. The left panel shows numerical solutions of the ordinary differential equations together with the agent based simulation. The ODE solution is represented with dotted lines and a single typical agent based simulation is represented with the solid lines. The different colors represent the number of cells infected with the respective number of copies of the virus. The right panel shows a comparison of agent based simulations for two neutral virus strains (upper right panel) versus two non-neutral strains (lower right panel). In the neutral case, drift is observed with the eventual fixation of one of the virus strains. In the non-neutral case, we assume that strain A has higher fitness over strain B. As a result, strain A will fixate.

Figure S4 shows snapshots of a typical stochastic spatial simulation with infection by a single virus strain. The left panels show a simulation which includes only free virus transmission, whereas the right panels show a simulation which includes only cell-to-cell transmission. The top panels show the status of each grid point, where red grid points denote infected cells. The bottom panels show the multiplicity of infection of each cell, with darker colors representing higher multiplicity. While non-spatial free virus transmission leads to mostly singly infected cells uniformly spread out across the grid, we see here that cell-to-cell transmission leads to spatial clumps of superinfected cells. This is because cell-to-cell transmission leads to the repeated infection of nearby cells, where each time an infection events occurs, multiple copies of the virus are passed.

2 Generation of double mutants

In this section we show that a combination of free virus and cell-to-cell transmission results in faster generation of double mutants by recombination. To study double-hit mutant generation, we ran the simulation repeatedly and recorded the time at which the double mutant was first generated,

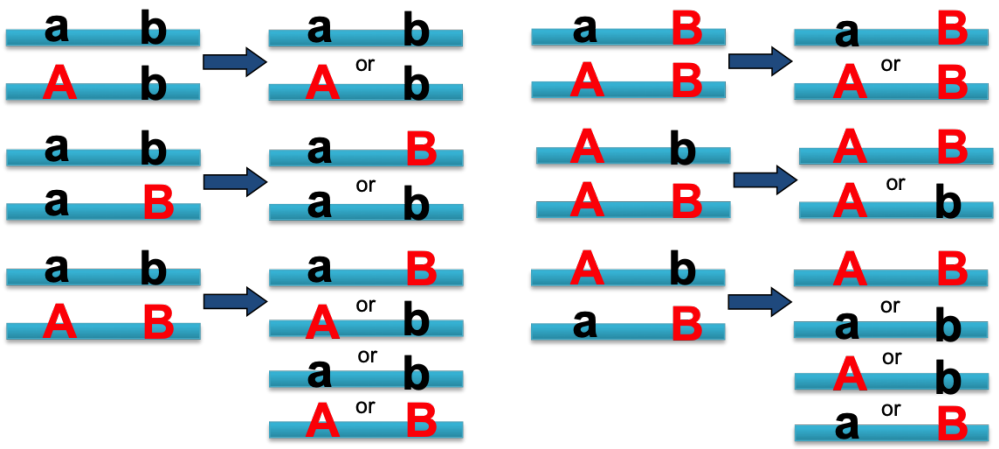

Figure S2: All recombination possibilities between the types, including when the infecting strand is the same as one of the parental strands. If the two strands are of the same strain then recombination is trivial. We define the recombination rate ρ as the probability that a new exchange happens between the strands, and the resulting infecting strand is different from both of the parental strands. This is because the most interesting recombination events are when $ab + AB \rightarrow Ab$ or aB and when $Ab + aB \rightarrow ab$ or AB. For this reason, the recombination rate ρ is capped at $\frac{1}{2}$ in the context of our agent-based model.

at which point the simulation was terminated. The average time of double mutant generation for various combinations of synaptic and free virus transmission is shown in figure S5.

In the absence of recombination, double mutant generation occurs fastest with purely synaptic transmission and takes longer as the contribution of free virus transmission is increased. This is because each time a synaptic infection event occurs, multiple viruses are transferred from the source cell to the target cell, thus increasing the number of mutation events that can occur during reverse transcription.

In the presence of recombination, however, we observe that double mutant generation occurs fastest for a mixture of free virus and synaptic transmission (figure S5). The reason is the existence of a tradeoff. Free virus transmission is efficient at bringing together two distinct virus strains (single mutant A and single mutant B) in the same cell, which is essential for recombination (creating the double hit mutant) to occur. Once in the same cell, however, the two virus strains are likely to disperse to different target cells rather than being repeatedly co-transmitted, which limits opportunities for recombination. In contrast, synaptic transmission promotes the co-transmission of two different virus strains once they have come together into the same cell [6], which generates more opportunities for recombination to occur. At the same time, however, the spatial nature of this process makes it less likely that they come together in the same cell to start with. The observed optimum thus presents the best solution to this tradeoff.

The same general trends hold if both one-hit mutants and double mutants are advantageous or disadvantageous (not shown).

3 Dynamics of mutant generation and spread

In this section we provide details of modeling generation and spread of double hit mutants, both advantageous and disadvantageous.

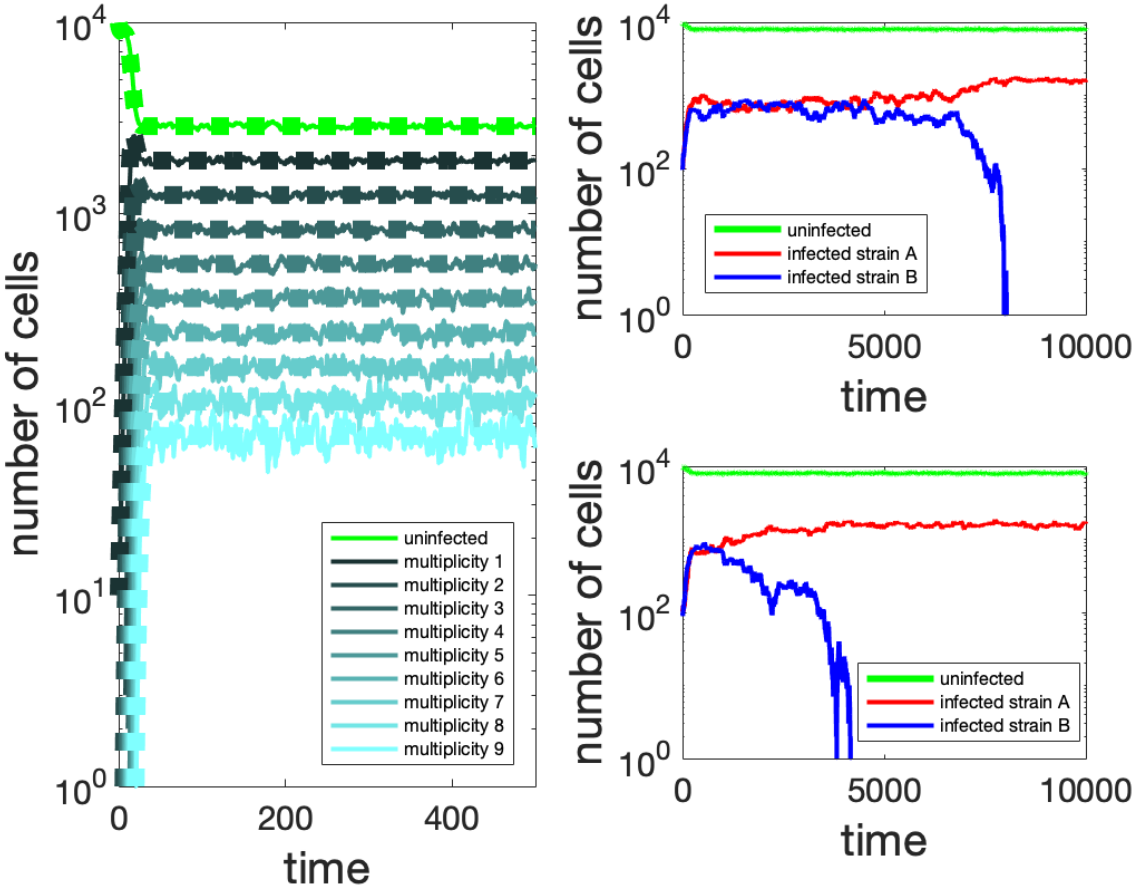

Figure S3: Left: comparison of the ODE, equations (7-8) (dotted lines), and agent based models (solid lines) for infection with a single strain. The numerical solutions for the ordinary differential equations match the agent based simulation and equilibrium values for each virus population. Here we include only free virus transmission, and parameters are $N = 9$, $\lambda = 0.88$, $\beta = 0.7$, $\gamma = 0$, $a = 0.2$, $d = 0.1$ and $\mathcal{N} = 100$. We initialize the grid by including an uninfected cell at each grid point. Right: comparison of agent based simulations for two neutral virus strains versus two non-neutral strains. Here we include only free virus transmission, and parameters are $\lambda = 0.5$, $\beta = 0.1$, $\gamma = 0$, $a = 0.08$, $d = 0.01$ and $\mathcal{N} = 100$. We initialize the grid by including an uninfected cell at each grid point. Above: neutral virus strains with the same fitness. Below: strain A has higher fitness over strain B. The fitness of strain A is 1 and the fitness of strain B is 0.95.

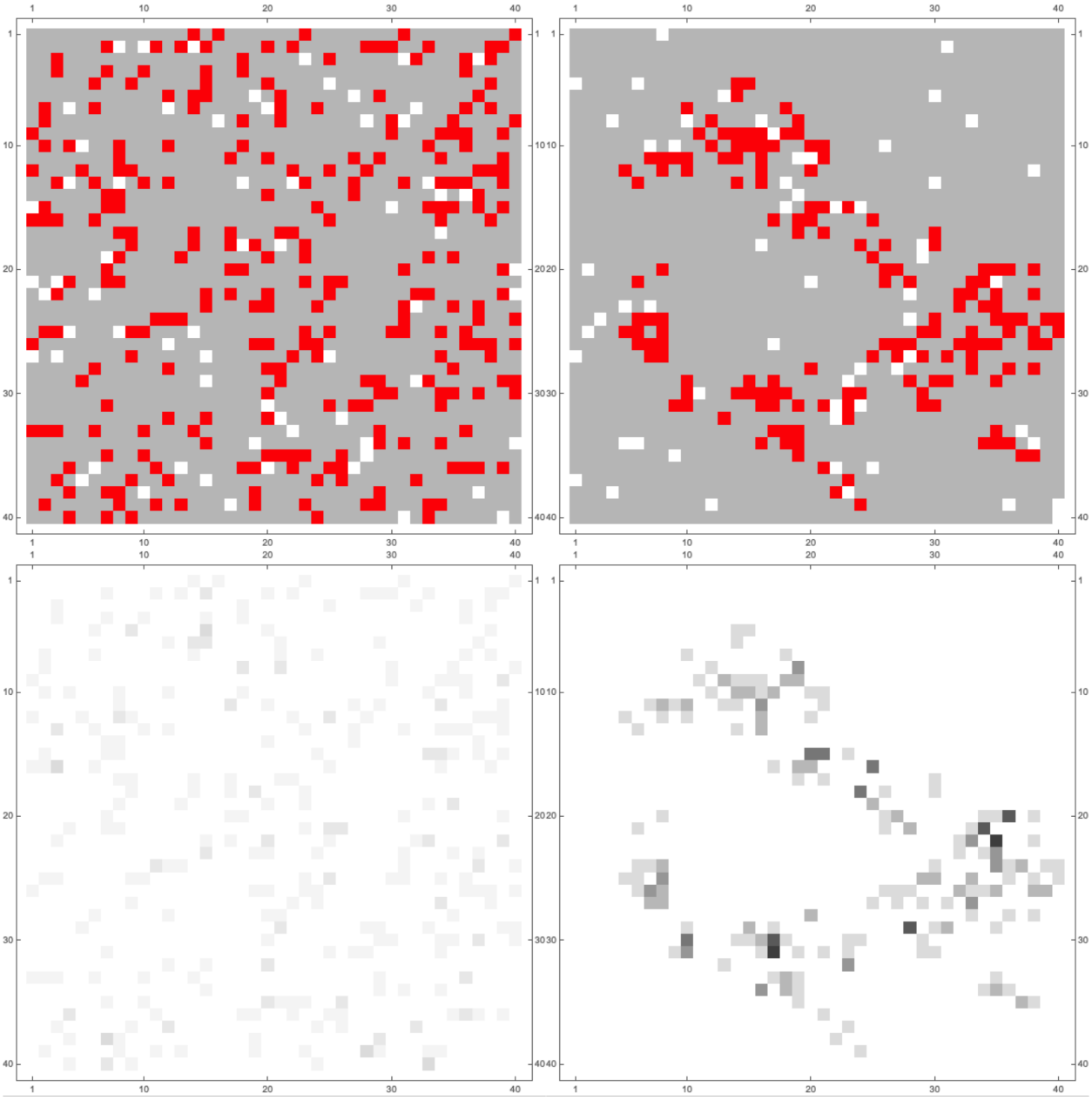

Figure S4: Example of stochastic simulations on a 40 by 40 grid at time $T = 100$. The panels on the left correspond to the same simulation with only free virus transmission. The panels on the right correspond to the same simulation with only synaptic cell-to-cell transmission. The panels on top show the infection where white grid points are empty, gray grid points are uninfected cells, and red grid points are infected cells. The panels on the bottom show the number of copies of virus each cell is infected with, where darker colors represent higher numbers. Other parameters are $\lambda = 0.5,\ \beta + \gamma = 0.1,\ a = 0.08,\ d = 0.01$, and $S = 3$.

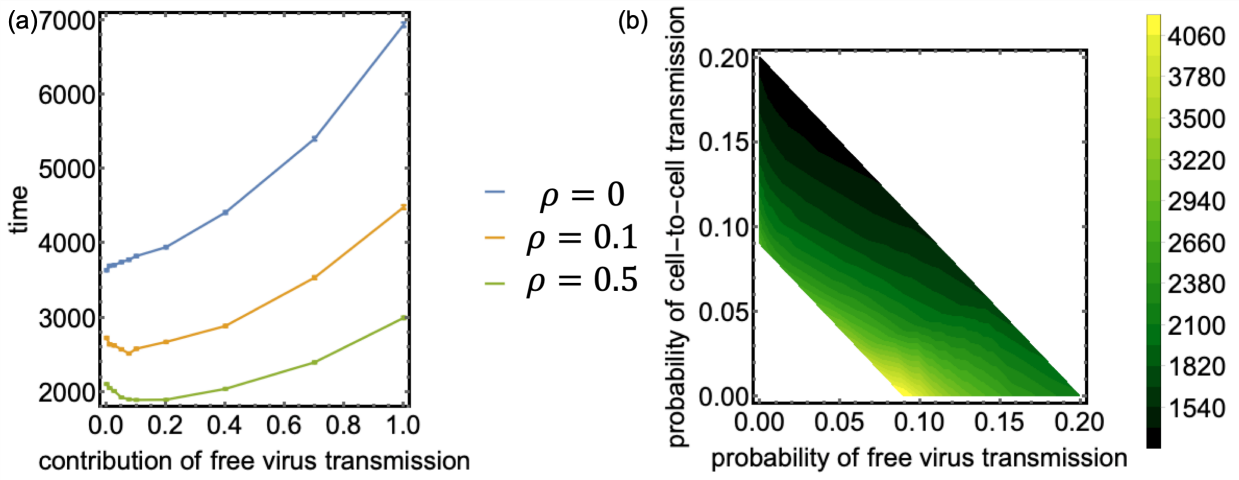

Figure S5: Generation of double mutants. (a) Time to double mutant generation, as a function of the rate of synaptic transmission, with $\beta + \gamma = 0.1$. Higher recombination rates lead to faster times to first double hit mutant generation. Standard error bars are shown. Each point represents the average over at least 12,280 runs. With a positive recombination rate $\rho \gg \mu$ a combination of free virus and cell-to-cell transmission optimizes the time to first double hit mutant generation. (b) Contour plot for the time to recombinant, plotted against the probability of free virus transmission (β) and the probability of cell-to-cell transmission (γ). Darker colors represent faster (lower) time to the creation of a recombinant virus. Diagonal lines with slope -1 and intercept c represent fixed $\beta + \gamma = c$. For fixed c, a combination of both free virus (β) and cell-to-cell transmission (γ) minimizes the time to the creation of recombinant virus. Contour plot was made by running the simulations for many points on the lines with fixed c for $c \in [0.09, 0.2]$ (for $c < 0.09$, the simulated infections go extinct with relatively higher probabilities). We used $\rho = 0.2$; enough simulations were run such that the averages with their respective standard error did not overlap. Other parameter values are $S = 3,\ \lambda = 1,\ d = 0.01,\ a = 0.02,\ \mathcal{N} = 100,\ \mu = 3 \times 10^{-5}$, and we initially infect randomly with only the wild type.

3.1 Advantageous mutants: the time series

In the case of advantageous mutants, a reasonable measure of double mutant success is the time it takes for the double hit mutant to reach 90% of all infected cells. Figure S6 presents examples of typical infection dynamics with (right) and without (left) recombination, both for relatively low (top) and high (bottom) mutant advantage. We can see that at first, populations of single mutants rise, and at some point produce a double hit mutant, which eventually rises to domination, displacing other populations. Parameters of the system define the typical timing of this process.

In the presence of double hit mutant advantage, the following factors trade-off to determine where recombinations boost or suppress double mutant spread: (i) the constructive force of double hit mutant creation by recombinations (which enhances double hit mutant production), (ii) the destructive force of recombination that breaks down double mutants (which delays double mutant spread); and (iii) the strength of selection of the double mutant, which defines the how long the previous two factors are at play.

Consider the case where the mutant advantage (s) is relatively low (figure S6, top panels). For a stretch of time, two single mutant strands coexist in the population at low levels. During this period, in the absence of recombinations, a double hit mutant is created by mutations and eventually rises to domination. In the presence of recombination, double hit mutants are created at a faster rate through recombinations between single strand mutants, but since the advantage is low, they remain at low levels for a long time, which contributes to frequent breakage events through recombinations with the abundant wild type. This destructive force of recombinations is what makes recombinations delay the domination of double hit mutants.

When the mutant advantage is relatively high (figure S6, bottom panels), all the same processes take place, but their relative contributions shift. Once a double hit mutant is created, it rises relatively fast due to larger selection force, leaving the "breaking" recombinations less time to operate. On the other hand, recombinations between the two single strains still accelerate double mutant production, thus resulting in a net positive, accelerating effect of recombination on double hit mutant domination dynamics.

3.2 Measuring the level of disadvantageous mutants

In the disadvantageous mutant scenario, mutant populations are less fit than wild-type viruses and do not invade. Rather, they steadily approach a balance between selection and mutation. Thus, in the long run, the double mutants converge to fluctuating around an equilibrium, the magnitude of which is determined by the mutation rate and the degree of the selective disadvantage. In the main text, a measure of double mutant relative abundance is used to assess its prominence.

To measure the relative abundance, we numerically determined the average double mutant fraction at an arbitrary time point $T = 10^5$ over many simulation runs. However, we also developed a different measure of double mutant success that yields very similar results. This measure is a temporal moving average for a single run, rather than considering averages at a fixed time point over many runs. Here, only one simulation is done at each parameter combination. The temporal moving average is calculated by (i) determining the relative fraction of cells infected with the double mutant over the total number of infected cells at each time step and then (ii) calculating the average of this fraction over the number of time steps elapsed. If the infection dies out (which only happens very rarely), results from that simulation are discarded and a new, more typical simulation is used.

The advantage of this approach is that only a single simulation is needed at each combination.

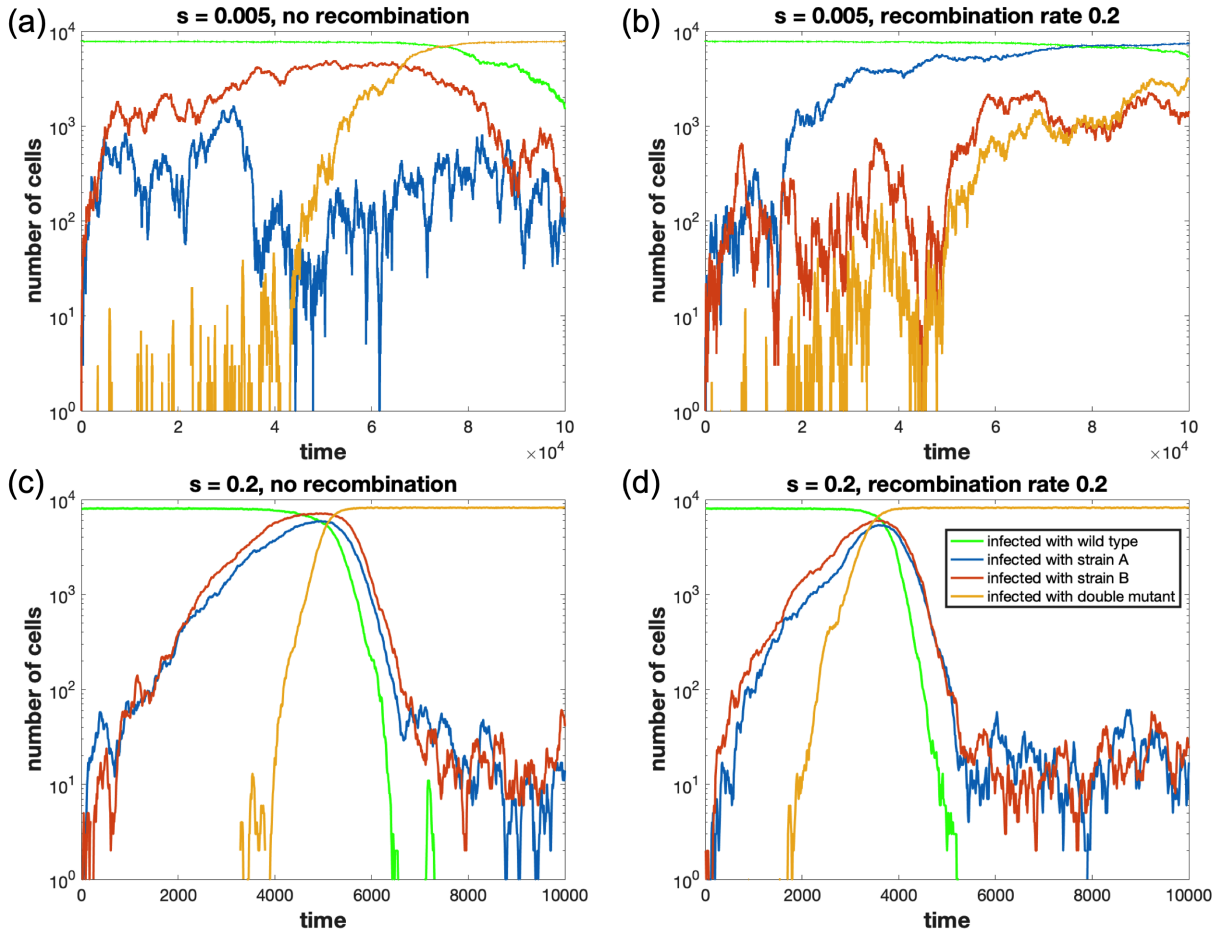

Figure S6: Advantageous mutants: the dynamics of cell populations, typical time-series. (a): slight advantage $s = 0.005$, no recombination $\rho = 0$ (b): slight advantage $s = 0.005$, recombination rate $\rho = 0.2$ (c): large advantage $s = 0.2$, no recombination $\rho = 0$ (d): large advantage $s = 0.2$, recombination rate $\rho = 0.2$. The other parameters are: $S = 3$, $\lambda = 1$, $\beta + \gamma = 0.1$, $d = 0.01$, $a = 0.02$, $\mathcal{N} = 100$, $\mu = 3 \times 10^{-5}$, $\alpha = 0.75$, 40% free-virus transmission, and initial infection with only the wild type at equilibrium levels.

The disadvantages are that (i) single simulations need to run to at least the 10^6 time step (ii) the fraction of double mutant abundance needs to be calculated at each time step (slowing the speed of the simulation) and (iii) this measure only has relevance when a selection mutation balance is achieved. In the neutral case, when only drift occurs, this measure is not useful.

3.3 Using ODEs to study selection mutation balance

As stated in the previous section, in the case of disadvantageous mutants, mutant populations are maintained by a balance between selection and mutation. It is reasonable to use ODEs to approximate this balance, and to determine whether or not recombination is a helpful force in the spread of the double hit mutant population.

The presence of recombination results in a more complex dependence between double-hit mutant creation and destruction, which can promote its spread. The key is the abundance of the single-hit mutants, compared to the abundances of double mutants and the wild types. Let us denote the abundance of single mutants of type A (or B) as at time t as Y_1, and the abundances of double mutants and the wild types as Y_2 and Y_0 respectively. From Supplemental Figure S2, the rate of "breaking" recombinations, is

$$\rho(3/4)Y_0Y_2 + \rho(1/2)Y_1Y_2 + \rho(1/2)Y_1Y_2.$$

Similarly, from Supplemental Figure S2, the rate of "making" recombinations, is

$$\rho(1/4)Y_0Y_2 + \rho(1/4)Y_1Y_1 + \rho(1/2)Y_1Y_2 + \rho(1/2)Y_1Y_2.$$

Therefore, by setting these expressions equal to one another, we have balance at time t if

$$Y_1^2 = 2Y_0Y_2. \tag{9}$$

If the left hand side of (9) is larger, then recombination between single mutants is more likely, which leads to the net creation of double mutants. If the right hand side of (9) is larger, then most recombination events will destroy the double mutant through recombination with wild-type, leading to the net loss of double mutants.

To implement these ideas, we use ODEs that do not explicitly include recombination. Instead, we look at the balance of $Y_1^2 = 2Y_0Y_2$ at time T in an ODE system without recombination (thus neglecting all recombination events up to time T).

To define the ODE system, we assume the same 4 strains, where each strain can (forward or back) mutate at site a/A and/or at site b/B during each infection event. Let $x_{i,j,k,l}(t)$ be the number of cells infected with i copies of wild type, j copies of mutant strain A, k copies of mutant strain B, and l copies of the double mutant at time t. Let W, A, B, D be the density of all populations infected with the wild type, mutant strain A, mutant strain B, and double hit mutant AB respectively at time t, that is

$$\begin{aligned}
W(t) &= \sum_{0<i+j+k+l\leq N} \frac{i}{i+j+k+l} x_{i,j,k,l}(t), \\
A(t) &= \sum_{0<i+j+k+l\leq N} \frac{j}{i+j+k+l} x_{i,j,k,l}(t), \\
B(t) &= \sum_{0<i+j+k+l\leq N} \frac{k}{i+j+k+l} x_{i,j,k,l}(t), \\
D(t) &= \sum_{0<i+j+k+l\leq N} \frac{l}{i+j+k+l} x_{i,j,k,l}(t).
\end{aligned}$$

Let Z be the sum of all infected populations. We then have that

$$Z(t) = \sum_{0<i+j+k+l\leq N} x_{i,j,k,l}(t) = W(t) + A(t) + B(t) + D(t).$$

The wild type mutates into mutant strain A with probability $\mu(1-\mu)$, which represents mutation at point A and no mutation at point B. Similarly, the wild type mutates into mutant strain B with probably $(1-\mu)\mu$ and into the double mutant with probability μ^2. This means the wild type does not mutant with probability $1-2\mu+\mu^2$. Similar mutation probabilities follow for the other strains. The ODE system is

$$x_{0,0,0,0} = \lambda(\mathcal{N}^2 - Z - x_{0,0,0,0}) - \frac{\beta}{\mathcal{N}^2} Z x_{0,0,0,0} - \frac{\gamma}{\mathcal{N}^2} Z x_{0,0,0,0} - d x_{0,0,0,0} \tag{10}$$

$$\begin{aligned} x_{i,j,k,l} &= \frac{\beta}{\mathcal{N}^2}\Big(f_W(W(1-2\mu+\mu^2) + A(\mu(1-\mu)) + B((1-\mu)\mu) + D(\mu^2)) x_{i-1,j,k,l} \\ &+ f_A(W(\mu(1-\mu)) + A(1-2\mu+\mu^2) + B(\mu^2) + D((1-\mu)\mu)) x_{i,j-1,k,l} \\ &+ f_B(W((1-\mu)\mu) + A(\mu^2) + B(1-2\mu+\mu^2) + D(\mu(1-\mu))) x_{i,j,k-1,l} \\ &+ f_D(W(\mu^2) + A((1-\mu)\mu) + B(\mu(1-\mu)) + D(1-2\mu+\mu^2) x_{i,j,k,l-1} - Z x_{i,j,k,l}\Big) \\ &+ \frac{\gamma}{\mathcal{N}^2}\Big(f_W(W(1-2\mu+\mu^2) + A(\mu(1-\mu)) + B((1-\mu)\mu) + D(\mu^2)) x_{i-S,j,k,l} \\ &+ f_A(W(\mu(1-\mu)) + A(1-2\mu+\mu^2) + B(\mu^2) + D((1-\mu)\mu)) x_{i,j-S,k,l} \\ &+ f_B(W((1-\mu)\mu) + A(\mu^2) + B(1-2\mu+\mu^2) + D(\mu(1-\mu))) x_{i,j,k-S,l} \\ &+ f_D(W(\mu^2) + A((1-\mu)\mu) + B(\mu(1-\mu)) + D(1-2\mu+\mu^2) x_{i,j,k,l-S} - Z x_{i,j,k,l}\Big) - a x_{i,j,k,l} \end{aligned} \tag{11}$$

where any population with a negative index is 0 and infection does not occur if it would result in a cell being infected with more than maximum infection multiplicity N viruses.

In order to evaluate whether recombination is beneficial for a given parameter set and fitness landscape, we calculate the number of each type of virus in the system at time $T = 10^5$. If $Y_1^2 > 2Y_0Y_2$ then recombination is beneficial, otherwise it is not. The predictions from the ODE system do not perfectly match the results from the stochastic system because of many factors, including (i) the ODEs do not take into account the spatial nature of cell-to-cell transmission, (ii) the ODEs are deterministic, (iii) recombination is neglected until time T, and (iv) a maximum infection multiplicity N must be used in order to solve the ODEs.

While they do not match perfectly, as seen in Figure S7 the ODEs do successfully qualitatively predict that for any parameter set with significant fitness difference s, recombination promotes double mutants under extreme negative epistasis (α close to 0) and suppresses them for extreme positive epistasis (α close to 1). This is again because for extreme positive epistasis, single mutants are less abundant, and "breaking" events dominate, resulting in recombinations suppressing double hit mutants. If on the other hand we have extreme negative epistasis, then the double hit mutants are extremely rare, and "making" events dominate, thus rendering recombination an enhancing force. The mathematical analysis of these ODEs and the differences between deterministic and stochastic simulations of these systems is an interesting question and a main topic of ongoing work.

4 A model with a lower multiplicity of infection

The model described in the main text is characterized by a relatively high equilibrium multiplicity of infection. Figure S8 shows a typical simulation where the mean multiplicity of all infected cells

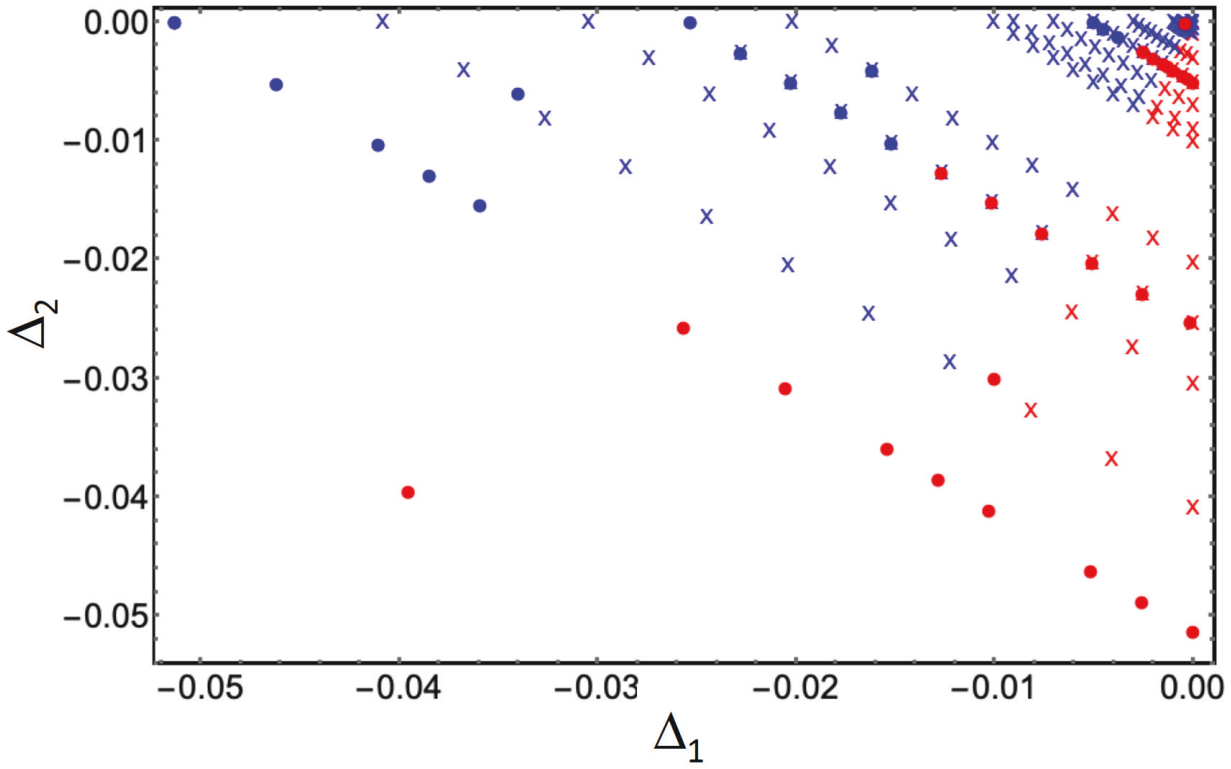

Figure S7: Results of the stochastic simulations (dots) versus the prediction from the ODE system (10-11) (crosses). The horizontal axis is Δ_1 and the vertical axis is Δ_2, which are the relative log fitness values of single and double mutants, respectively (compare to figure 1(c) of the main text). Red (blue) corresponds to runs where double hit mutants are more (less) abundant at $T = 10^5$ in simulations with recombinations than without. We assumed 40% free-virus transmission; the rest of the parameters are $S = 3,\ \lambda = 1,\ \beta + \gamma = 0.1,\ d = 0.01,\ a = 0.02,\ \mathcal{N} = 100,\ \mu = 3 \times 10^{-5},\ N = 30$ and initial infection with only the wild type at equilibrium levels.

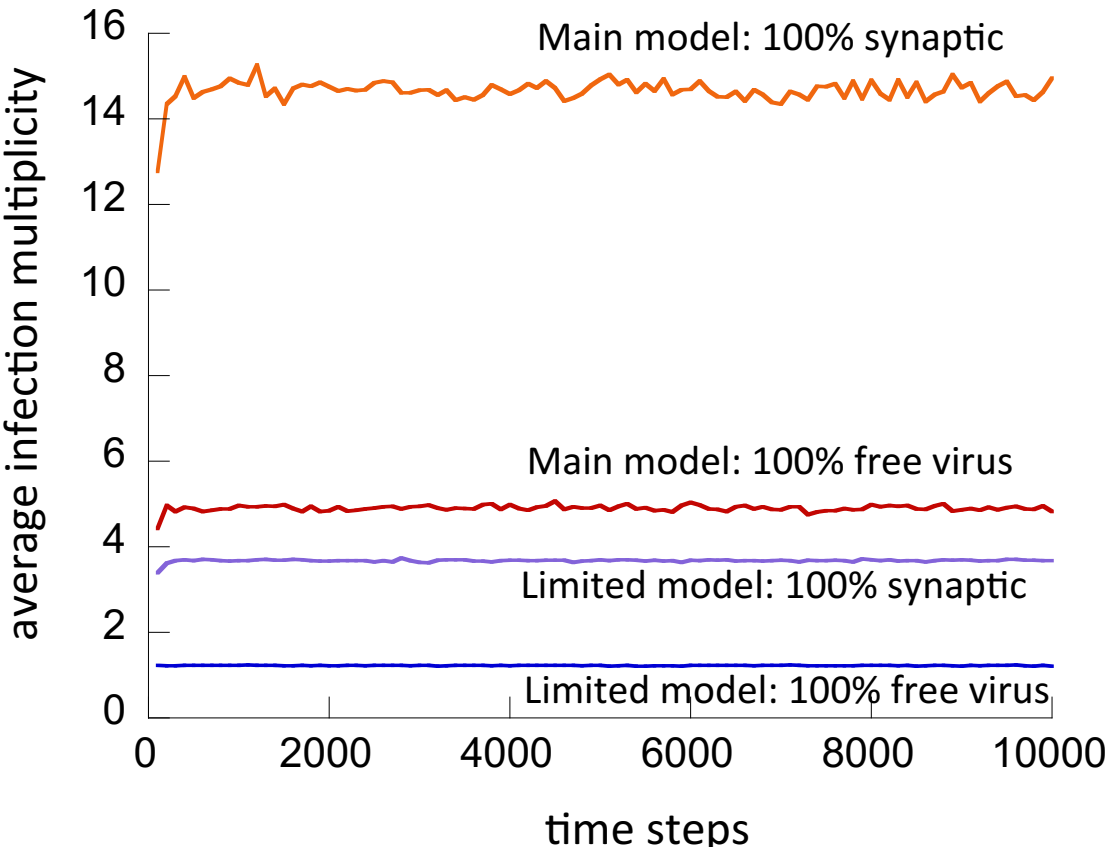

Figure S8: Mean multiplicity of infection as a function of time. The two top lines correspond to the model used in the main text (parameters as in figure 2 of the main text, except $\mu = 0$). The bottom two lines correspond to the limited multiplicity model, see figure S9. Results for synaptic only and free-virus only transmission are presented. Here we use $\nu = 0.5$.

is plotted as a function of time. We can see that for parameters used in figure 2 of the main text, under purely free virus transmission, a typical mean multiplicity of infection is about 4 viruses per cell, while under purely synaptic transmission, it is about 14 viruses per cell. In order to investigate how results change if infection multiplicity is lower, we designed a model with limited multiplicity. In this model, we keep track of the time, τ, that has passed since the first time a cell gets infected. The longer this time, the less likely it is that the cell gets superinfected. This is because after the initial infection, the virus eventually down-regulates the receptor required for viral entry, preventing further superinfection events from occurring [2]. We assumed that after the first infection event, each subsequent infection event for a given cell can be aborted with a probability $P = 1 - e^{-\nu\tau}$, which grows to its limiting value of 1 as τ increases. In this model, under purely free virus transmission, a typical mean multiplicity of infection is just slightly over one virus per cell, while under purely synaptic transmission, it is less that 4 viruses per cell, see figure S8.

Typical results of the limited multiplicity model are presented in figure S9. The patterns that are observed for the limited multiplicity model are very similar to those reported in the main text for the basic model.

Disadvantageous mutants. Simulations for disadvantageous mutants are presented in panels (a,b) of figure S9, and should be compared with figure 2(c,d) of the main text.

- For disadvantageous mutants under higher infection multiplicities, recombination increased

double mutant fractions at equilibrium under negative epistasis (panel (a)) and suppressed them under positive epistasis (panel (b)) if free virus transmission is dominant. This result is unchanged compared with the basic model.

- If synaptic transmission is dominant, we observed a reversal for higher multiplicities: recombination always increased double mutant fractions, even for positive epistasis. For low multiplicity, this reversal is not observed, i.e. double mutant levels are lower in the presence compared to the absence of recombination even at 100% synaptic transmission (figure S9(b)). We do find, however, that this reduction in double mutant levels in the presence of recombination is significantly less pronounced when synaptic transmission becomes more prevalent. Hence, the conclusion that synaptic transmission protects the double mutant against the detrimental effects of recombination continues to hold under low infection multiplicities.

- The larger the percentage of synaptic transmission, the higher the level of double mutants. This is similar to the basic model, and in some sense more pronounced, as this pattern holds for near 100% synaptic transmission.

Advantageous mutants. Simulations for advantageous mutants are presented in panels of figure S9 (c,d,e), and should be compared with figure 2(a,b) of the main text.

- For negative and zero epistasis, recombinations play an enhancing role in double mutant spread (panels (c,d)), as in the basic model.

- For large positive epistasis and a range of fitness advantage, recombinations become detrimental for double mutant spread (panel (e)), similar to the basic model. This effect, although statistically significant, is weaker in the limited multiplicity model compared to the basic model.

- The larger the percentage of synaptic transmission, the slower the spread of mutants. This is similar to the basic model, and in some sense more pronounced, as this pattern holds over all combinations of synaptic and free virus transmission.

Neutral mutants. Simulations for neutral mutants are presented in panel (f) of figure S9 and should be compared with figure 3(a) of the main text.

- Recombinations result in a higher level of double mutants, as in the basic model.

- A mixture of free virus and synaptic transmission is optimal for double mutant spread, as in the basic model.

5 Recombinations, epistasis, and transmission mode: additional information

5.1 The role of recombinations under different transmission modes

Figure S10 contains graphs supplementing Figure 4 of the main text, in the case of advantageous mutants. We show in the main text (figure 1(b) of the main text) that for advantageous mutants, under a mixture of free virus and synaptic transmission modes, recombinations mostly enhance double mutants except for a region of intermediate fitness advantages and relatively strong positive epistasis, where recombinations delay the spread of mutants.

It turns out that these results for advantageous mutants remain very similar under different mixtures of free virus and synaptic transmission. This is illustrated in figure S10, which show the

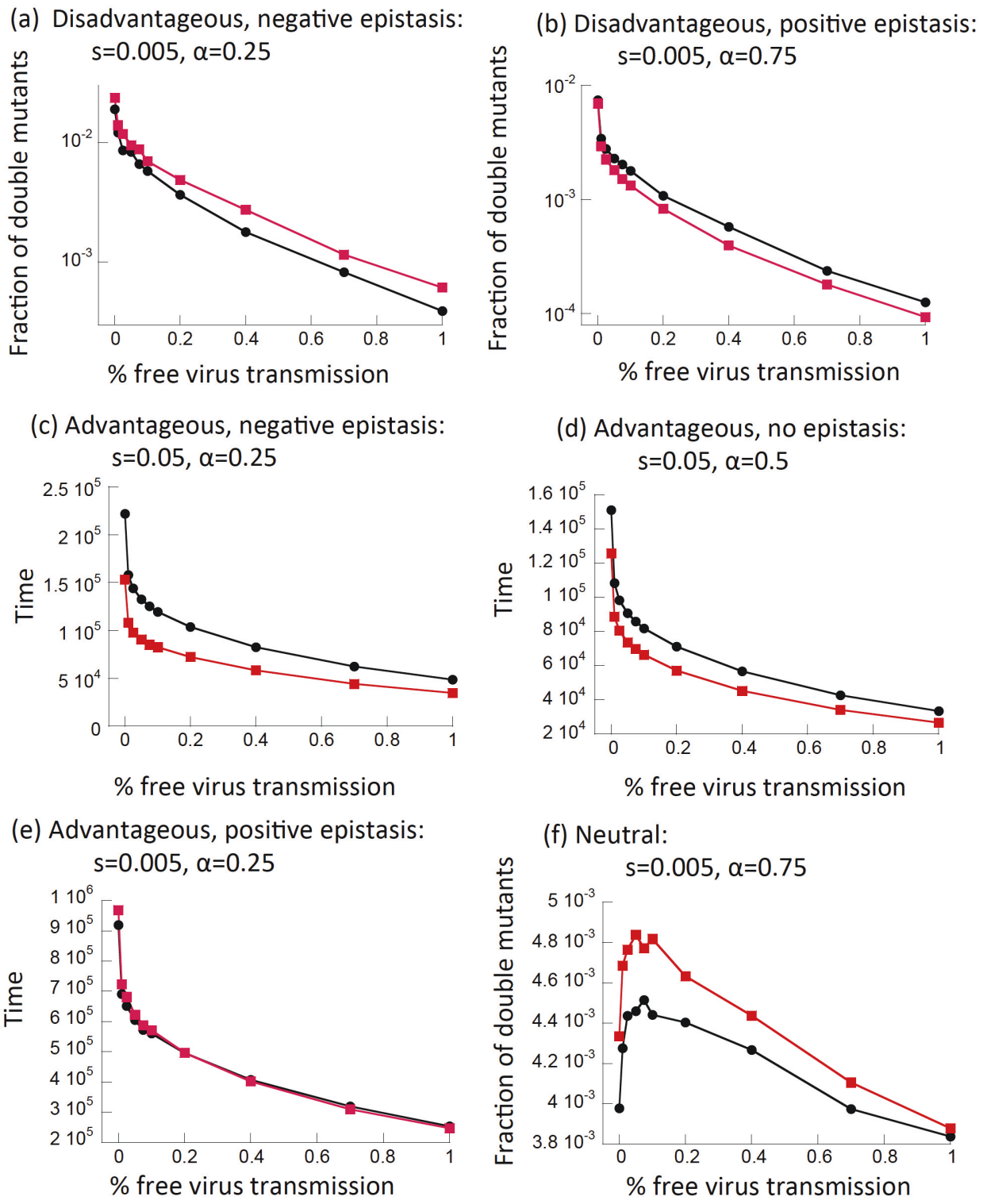

Figure S9: System with limited multiplicity: a comparison between models with (red) and without (black) recombination. (a,b) Disadvantageous mutants: the fraction of mutants (the temporal average at selection-mutation balance) as a function of the fraction of free virus transmission, under negative and positive epistasis (see figure 2(c,d) of the main text for other parameter values). (c,d,e) Advantageous mutants: the time until mutants reach 90%, for negative epistasis, no epistasis, and positive epistasis (see figure 2(a,b) of the main text for other parameter values). (f) Neutral mutants: the level of mutants as a function of the fraction of free virus transmission (see figure 3(a) of the main text for other parameter values). Vertical bars represent standard error and are too small to be seen. The additional parameter ν used in the limited multiplicity model was taken to be $\nu = 0.5$.

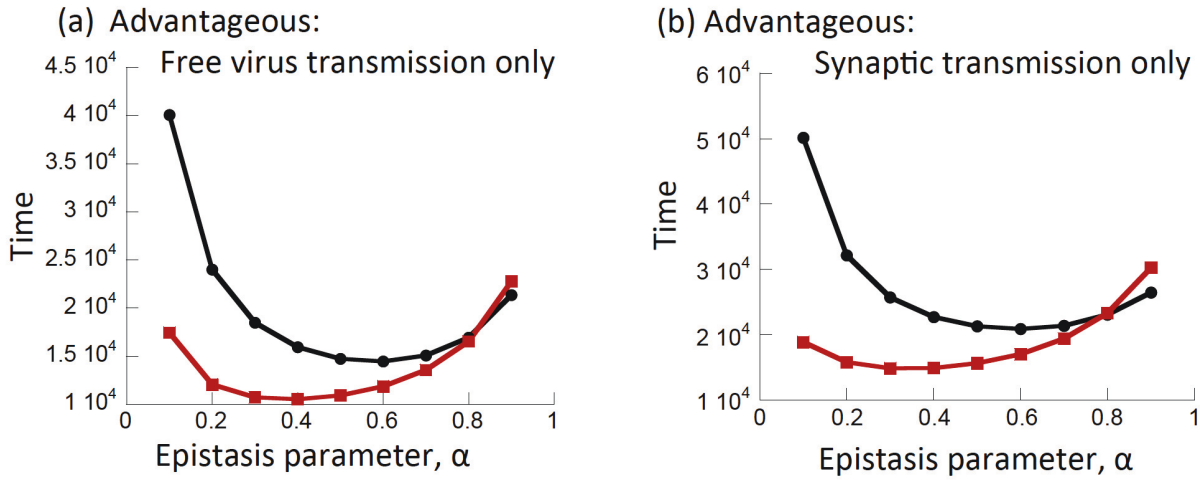

Figure S10: The role of recombinations under different transmission modes for advantageous mutants. Shown is the time for the double mutant to reach 90%. Red denotes simulations with recombination and black without recombinations. (a) Free virus transmission only, (b) synaptic transmission only. $s = 0.05$, and the other parameters are as in figure 2 of the main text. Each simulation was run at least 30,000 times. Error bars (based on standard errors) are plotted but are too small to see.

time to double mutant invasion with (red) and without (black) recombinations, under free virus transmission only (a) and under synaptic transmission only (b). The time of mutant spread is presented as a function of parameter α (where $\alpha < 0.5$ corresponds to negative epistasis and $\alpha > 0.5$ to positive epistasis). We can see that recombination becomes disadvantageous for mutants (by delaying the time of spread) for high values of α. In figure 1(b) of the main text, a similar outcome can be seen by looking along diagonal straight lines connecting points $\Delta_1 = A$ on the horizontal axis and $\Delta_2 = A$ on the vertical axis, where $A = |\ln(1-s)| = |\ln(1-0.05)| \approx 0.05129$.

Figure S11 contains graphs supplementing Figure 4 of the main text, in the case of disadvantageous mutants. In particular, panels (a) and (b) correspond to free virus transmission only and are similar to figure 4(a) of the main text, except they contain simulations for smaller ($s = 0.005$) and larger ($s = 0.075$) fitness disadvantage values compared to that of the main text ($s = 0.05$). Further, panels (c) and (d) correspond to synaptic transmission only ($\beta = 0$) and are similar to figure 4(b) of the main text; again, they correspond to a smaller and a larger fitness disadvantage. We observe that there is no qualitative differences for different values of fitness disadvantage.

5.2 Optimal epistasis to promote double mutants

Using the results presented above and in the main text, we can investigate what level of epistasis is optimal for double mutant spread, given the transmission mode, with and without recombinations.

Figure S10 suggests that for advantageous mutants, intermediate values of epistasis (α) are optimal to minimize the time until double mutant fixation. In order for the double mutant population to fixate past the 90% threshold, first the intermediate mutants need to overtake the wild type, and second the double hit mutant strain needs to overtake both of the intermediate mutant strains. For the mutants to quickly overtake the wild type, the intermediate mutant strains need to have a significant fitness advantage over the wild type, that is $\alpha < 1$. For the double mutant strain to quickly overtake the intermediate mutant strains, the double hit mutant needs to have a significant fitness advantage over the intermediate mutant strains, that is $\alpha > 0$. If the double hit

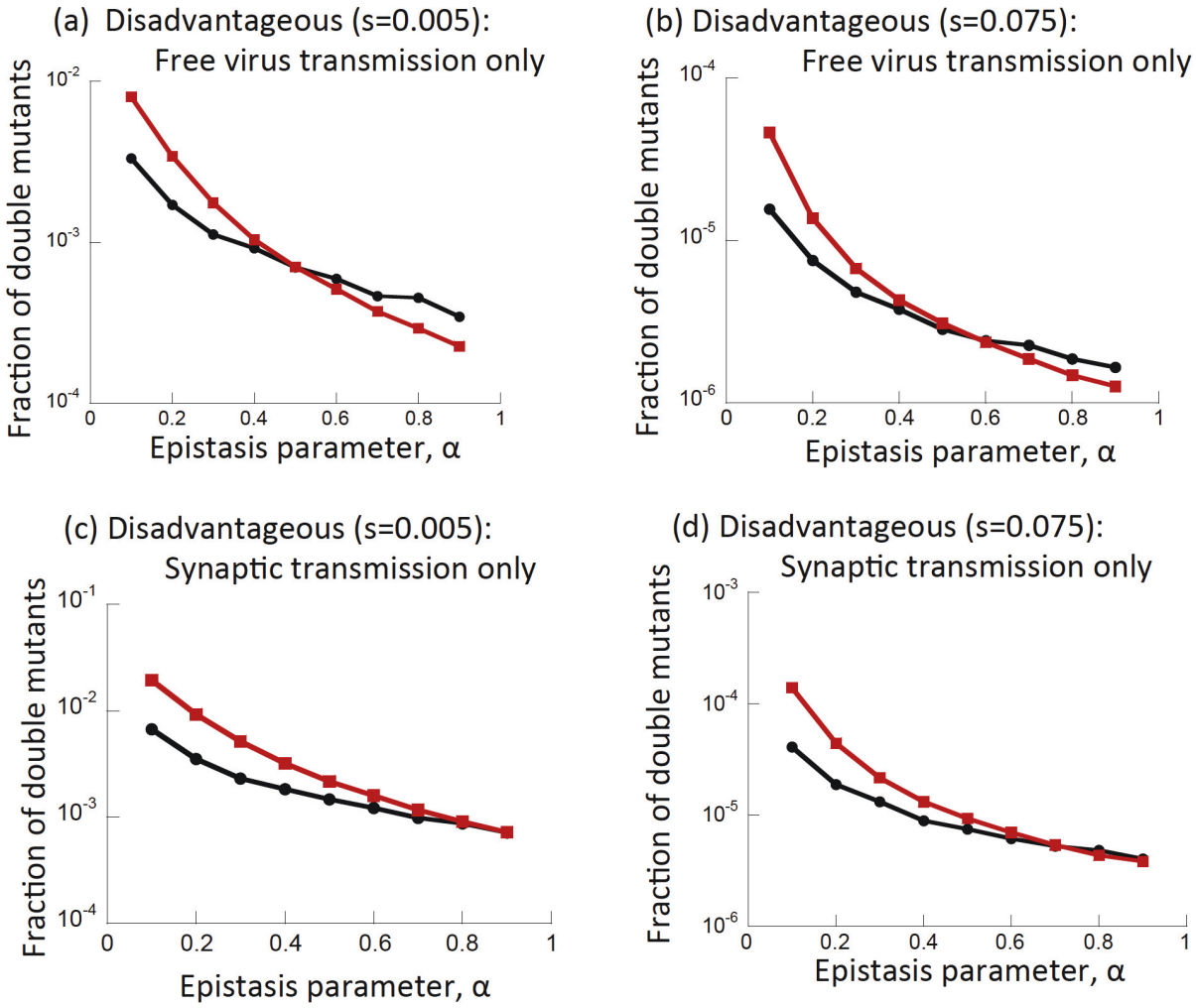

Figure S11: The role of recombinations under different transmission modes for disadvantageous mutants. Red denotes simulations with recombination and black without recombinations. (a,b) Free virus transmission ($s = 0.005$ and $s = 0.075$). (c,d) Synaptic transmission only ($s = 0.005$ and $s = 0.075$). Other parameters are as in figure 2 of the main text. The graphs show the temporal average of the double mutant at selection-mutation balance. Error bars (based on standard error) are plotted, but are too small to be visible.

mutant has no fitness advantage over the intermediate mutants, so $\alpha = 0$, all mutant strains have the same fitness and it takes longer for the double hit mutant strain to drift and fixate past the 90% threshold. This is true both in the absence and presence of recombination, and both under free virus and synaptic transmission. Figure S12 is a heat map showing this for a combination of free virus and synaptic transmission and a range of fitness differences s.

A different result is observed for disadvantageous mutants, see figure S11 and also figure 4 of the main text. As before, decreasing $\alpha \in [0, 1]$ leads to higher intermediate mutant fitness. On the other hand, decreasing α also leads to higher ratios of cells infected with the double hit mutant. This is because as the intermediate mutant fitness decreases, it becomes increasingly unlikely that the double hit mutant strain will be generated at all, either by mutation or recombination between the intermediate strains. Therefore, $\alpha = 0$ produces the largest level of double mutants. Again, this trend holds in the absence and presence of recombination, and both under free virus and synaptic transmission.

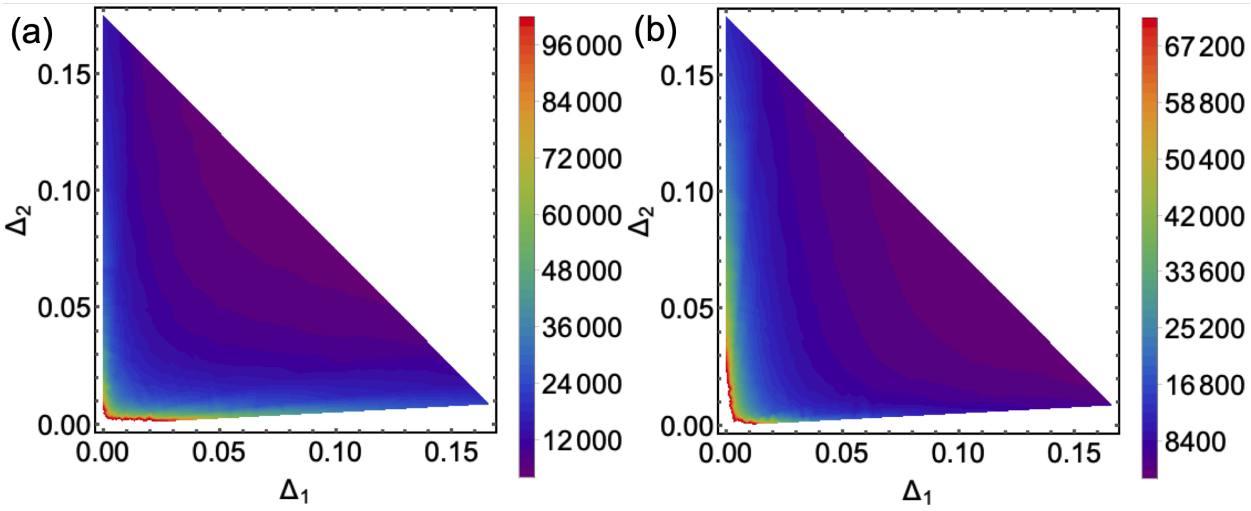

Figure S12: The optimal level of epistasis for double mutant spread. (a) Contour plot for the advantageous mutants with no recombination. The colors represent the time until double hit mutant fixation past a threshold of 90%. Lines with slope -1 and intercept $|\ln(1-s)|$ represent fixed s with $\alpha \in [0,1]$. Contour plots were made by running the simulations for many points on lines with fixed s for $s \in [0.001, 0.16]$. The total number of points is 517. The number of simulations at each point was chosen such that the averages with and without recombination with their respective standard error did not overlap. (b) Same with recombination rate $\rho = 0.2$. Other parameters are as in figure 2 of the main text.

5.3 Variation vs standard error

In the main text, figures 2 and 4 present the averages over many stochastic simulations for different conditions. Each average is plotted with a standard error bar, which is very small because of the large number of simulations. Here we show in figures S13 and S14 the same plots as in the main text figures 2 and 4 but plotted with the standard deviation instead of the standard error. The standard deviations are relatively large, which is typical for stochastic populations with small mutation rates. Statistical significance, however, depends on the number of simulations, which is expressed in the standard error. In general, the variation and standard deviation are larger in the absence of recombination.

5.4 Parameter values and robustness of the results

Simulation parameters used in our studies are defined in table 1, and their values/ranges are given. In this paper we performed a very systematic study of the role of (i) synaptic and/or free virus transmission (parameters γ and β), under (ii) different fitness landscapes (parameters s for advantage/disadvantage and α for epistasis), (iii) with and without recombination (parameter ρ). Hundreds of parameter combinations have been tested and comprehensive results presented.

Other parameters, however, were kept constant throughout most of this analysis, such as the production rate of uninfected target cells λ and death rate d of uninfected target cells, and the death rate a of infected cells. The value for the death rate of infected cells, $a = 0.02\text{hr}^{-1}$, was chosen to match the experimentally measured mean lifespan of HIV-infected cells of about 2 days, see [10]. Parameters λ, β, and d were selected to give the correct order of magnitude for R_0, as described in the main text.

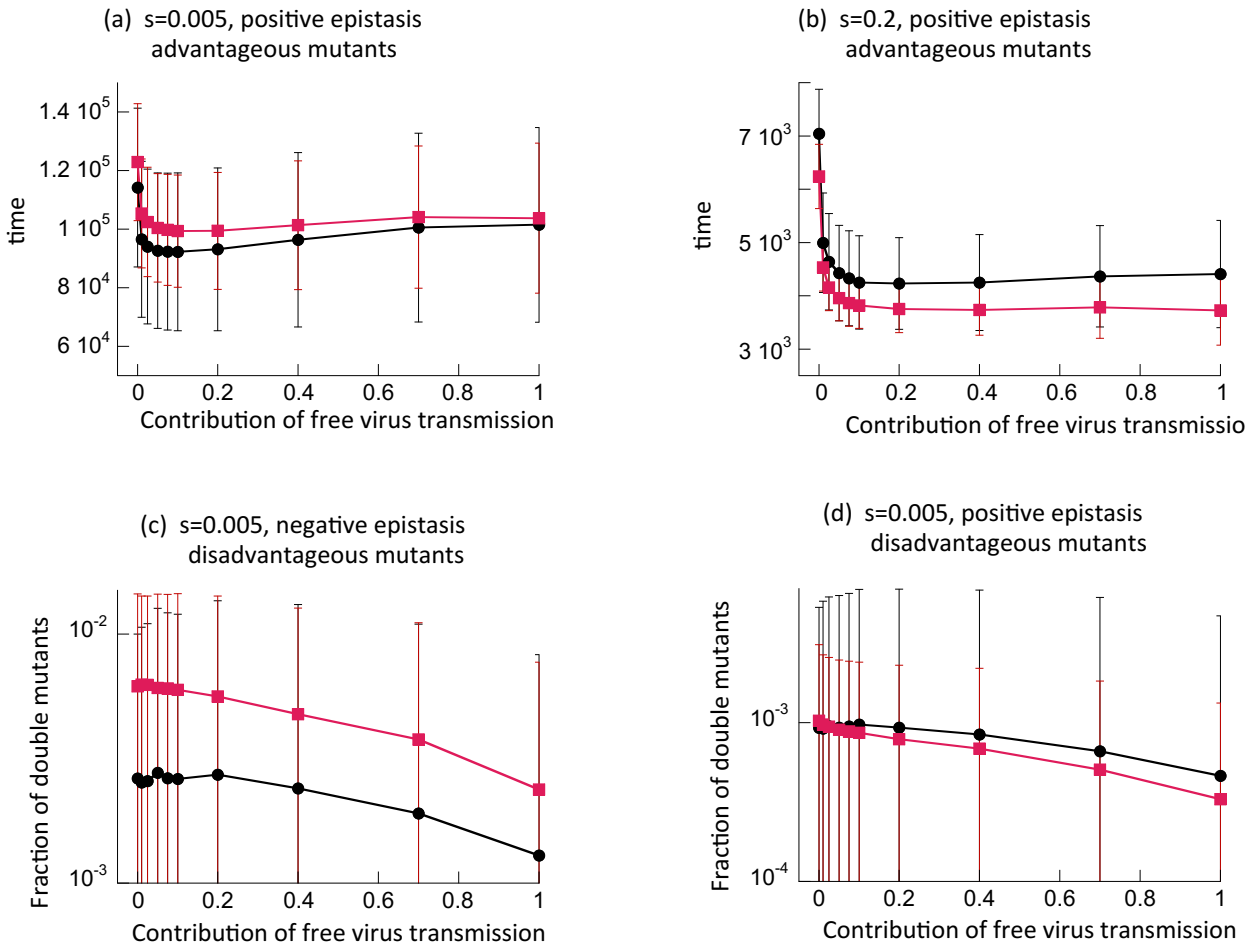

Figure S13: The role of recombination in (a,b) advantageous and (c,d) disadvantageous mutant dynamics. Red: with recombinations, and black: without recombination. (a-b) The time until the advantageous mutant reaches 90%, as a function of the fraction of free virus transmission. The means and standard deviation bars are shown. (a) $s = 0.005,\ \alpha = 0.75$. (b) $s = 0.2,\ \alpha = 0.75$. (c-d): The fraction of disadvantageous mutants at time $T = 10^5$, as a function of the fraction of free virus transmission. The means and standard deviation bars are shown. (c) $s = 0.005,\ \alpha = 0.25$ (d) $s = 0.005,\ \alpha = 0.75$. The parameters are: $\beta + \gamma = 0.1,\ S = 3,\ \lambda = 1,\ d = 0.01,\ a = 0.02,\ \mathcal{N} = 100,\ \mu = 3 \times 10^{-5}$. All averages are based on at least 10^4 simulations.

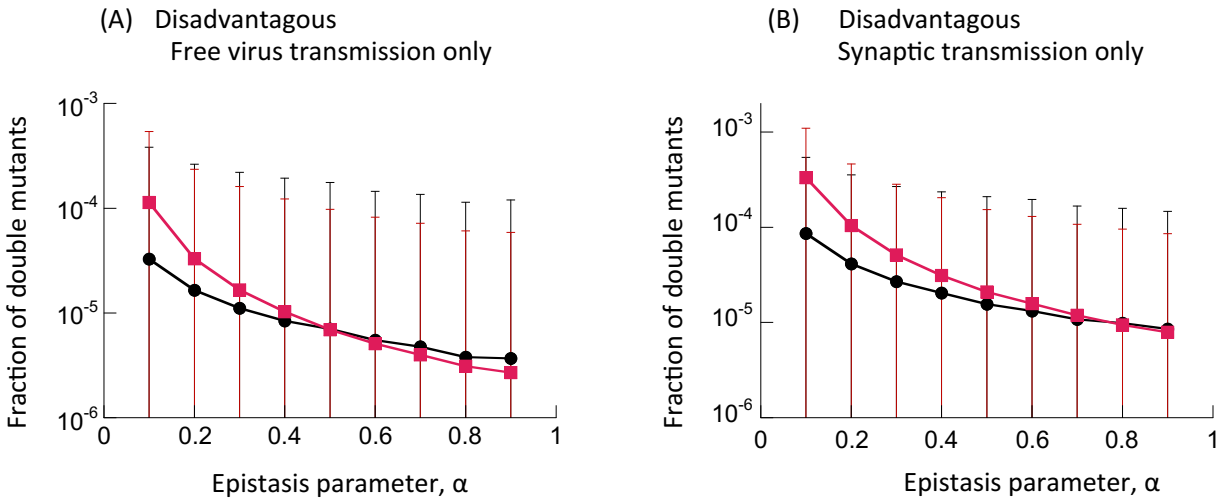

Figure S14: The role of recombinations under different transmission modes, for disadvantageous mutants. Shown is the temporal average of the fraction of double mutants at selection-mutation balance, as a function of that parameter α, defining the nature and extent of epistasis. Red denotes simulations with recombination and black without recombinations. (a) Free virus transmission only, (b) synaptic transmission only. $s = 0.05$, and other parameters are as in figure S13. Standard deviation bars are also plotted at each point.

Selective simulations with different values for these and other parameters have been performed, but we did not attempt an exhaustive analysis of the entire parameter space, due to the computational non-feasibility of this problem. Examples of alternative parameter values include: grid size $\mathcal{N} = 40$; $\lambda = 0.5\text{hr}^{-1}\text{vol}^{-1}$ and $\lambda = 0.88\text{hr}^{-1}\text{vol}^{-1}$; $d = 0.1\text{hr}^{-1}$; $a = 0.2\text{hr}^{-1}$ and $a = 0.08\text{hr}^{-1}$. In all simulations, qualitatively similar results are observed. We note here that a single value of the mutation rate, μ, was used, because this value is known for HIV [7]. Further, parameter S (the number of viruses transferred per synapse) was not varied (except setting it to $S = 1$ for comparison with the free-virus transmission model). Instead, to limit the mean multiplicity of infection, we used a superinfection regulation parameter, ν, which provided a more realistic and biologically based approach (see [1]) to achieve the same result as lowering S.

Notation	Description	Usual value/range (if applicable)
$\mathcal{N}$	linear size of agent-based model grid	100
λ	production of uninfected cells	$1.0\text{hr}^{-1}\text{vol}^{-1}$
d	death rate of uninfected cells	0.01hr^{-1}
a	death rate of infected cells	0.02hr^{-1}
β	rate of free virus transmission	$[0, 0.1]\text{hr}^{-1}\text{vol}^{-1}$, multiple values
γ	rate of synaptic cell-to-cell transmission	$[0, 0.1]\text{hr}^{-1}\text{vol}^{-1}$, multiple values
S	number of viruses transferred per synapse	3
μ	mutation rate	3×10^{-5}
ρ	recombination rate	$\{0, 0.1, 0.2, 0.5\}$
s	selection coefficient	$[0.001, 0.2]$, multiple values
α	epistasis parameter	$[0, 1]$, multiple values
ν	superinfection regulation parameter	$\{0, 0.5\}\text{hr}^{-1}$
γ_j^m	probability for a cell infected with m viruses to transmit j viruses per synapse	ODE model only
N	maximum infection multiplicity	ODE model only
ab	wild type strain	N/A
Ab and aB	single mutant strains	N/A
AB	double mutant strain	N/A

Table 1: Description of model parameters, symbols, and values/ranges. Curly brackets denote a set of several specific values used; square brackets denote a range, within which many values were used. For alternative values, see text.

References

[1] Benjamin K Chen, Rajesh T Gandhi, and David Baltimore. Cd4 down-modulation during infection of human t cells with human immunodeficiency virus type 1 involves independent activities of vpu, env, and nef. *Journal of virology*, 70(9):6044–6053, 1996.

[2] Narendra M Dixit and Alan S Perelson. HIV dynamics with multiple infections of target cells. *Proceedings of the National Academy of Sciences*, 102(23):8198–8203, 2005.

[3] Natalia L Komarova, David N Levy, and Dominik Wodarz. Effect of synaptic transmission on viral fitness in HIV infection. *PloS one*, 7(11):e48361, 2012.

[4] Natalia L Komarova, David N Levy, and Dominik Wodarz. Synaptic transmission and the susceptibility of HIV infection to anti-viral drugs. *Scientific reports*, 3:2103, 2013.

[5] Natalia L Komarova and Dominik Wodarz. Virus dynamics in the presence of synaptic transmission. *Mathematical biosciences*, 242(2):161–171, 2013.

[6] Kenneth M Law, Natalia L Komarova, Alice W Yewdall, Rebecca K Lee, Olga L Herrera, Dominik Wodarz, and Benjamin K Chen. In vivo HIV-1 cell-to-cell transmission promotes multicopy micro-compartmentalized infection. *Cell reports*, 15(12):2771–2783, 2016.

[7] Louis M Mansky and Howard M Temin. Lower in vivo mutation rate of human immunodeficiency virus type 1 than that predicted from the fidelity of purified reverse transcriptase. *Journal of virology*, 69(8):5087–5094, 1995.

[8] Martin Nowak and Robert M May. *Virus dynamics: mathematical principles of immunology and virology*. Oxford university press, 2000.

[9] Alan S Perelson. Modelling viral and immune system dynamics. *Nature Reviews Immunology*, 2(1):28, 2002.

[10] Alan S Perelson, Avidan U Neumann, Martin Markowitz, John M Leonard, and David D Ho. Hiv-1 dynamics in vivo: virion clearance rate, infected cell life-span, and viral generation time. *Science*, 271(5255):1582–1586, 1996.

[11] Jun Seita and Irving L. Weissman. Hematopoietic stem cell: self-renewal versus differentiation. *WIREs Systems Biology and Medicine*, 2(6):640–653, 2010.